UNIVERSITÉ D'OTTAWA
UNIVERSITY OF OTTAWA

DETECTION OF N.M.R. USING A SUPERCONDUCTING QUANTUM INTERFEROMETRIC DEVICE

by

R.G. Goodchild

Submitted to the School of Graduate Studies
in partial fulfilment of the requirements
for the degree of Master of Science

Department of Physics
Faculty of Science and Engineering
The University of Ottawa
Ottawa, Canada

1975

ABSTRACT

A magnetometer, utilizing a SQUID, has been constructed and used to study the N.M.R. signal amplitude of Cu^{63} as a function of r.f. power, as well, the relaxation time of the F^{19} nuclear spin system in CaF_2 for a magnetic field range of 3.0 - 30.0 mT is investigated.

The former, is a preliminary step towards the construction of an N.M.R. thermometer for the temperature range below 4.2K and several aspects relating to this problem are discussed. The latter, is an investigation into the use of such a magnetometer for the study of long relaxation times in insulators.

ACKNOWLEDGMENT

The author wishes to thank Dr. G. Lamarche for his interest and assistance in this work; Drs. C. Benson and A. Manoogian; B. Hébral, P. Rochon, A. Leclerc, J. Davoine, M. O'Connell and J. O'Sullivan, for their assistance and many inspiring discussions.

He also thanks C.N. Goodchild and R.W. Knott, for their excellent work on the magnetometer head; Mrs. C. Goodchild for the typing of this thesis and finally...

Susan F. Cox, devil's advocate.

TABLE OF CONTENT

LIST OF FIGURES

LIST OF GRAPHS

INTRODUCTION

The work described herein originates from an interest in a new instrument called SQUID (Superconducting QUantum Interferometric Device), which has been commercially available since 1970[1]. The instrument, based on London's concept of fluxoid quantization in a superconductor and on Josephson tunneling through a weak link between two superconductors, is essentially a quantum flux counter that allows, among other things, the realization of a magnetometer with an unprecedented sensivity approaching 10^{-19} Wb.

We were primarily interested in exploiting the new possibilities offered by the SQUID Magnetometer (S.M.) in bio-magnetism and nuclear magnetism. It has been demonstrated by Cohen[2], Rosen et al[3], and Zimmerman and Frederick[4], that the S.M. is capable of detecting the time varying magnetic fields that accompany heart and cerebral activity. In fact, these groups succeeded in producing Magneto-Cardiograms (MCG) and Magneto-Encephalograms (MEG) of a quality comparable to the more familiar ECG and EEG. The point of interest is that the MCG and MEG were obtained without any physical contact to the patient. Our interest in bio-magnetics was in observing the magnetic field accompanying nerve impulses transmitted in a single nerve cell. The usual procedure makes use of probes embedded in the tissue. Thus, the S.M. would allow measurements without disruption of the cell. A preliminary investigation of this problem was presented at a meeting of ACFAS in 1974 and will not be further discussed.

The interest in S.M. as an instrument for the detection of nuclear magnetism, comes in part from the possibility of using the property for low temperature thermometry. Indeed an assembly of nuclei having a non-zero magnetic moment behaves like a paramagnetic gas and is expected to follow Curie's law rigorously down to at least 0.1 mK. This represents an ideal thermometer providing thermal equilibrium can be established with the substance under investigation. Metallic samples present the best possibilities for thermal conduction and fast attainment of thermal equilibrium at very low temperatures and have been investigated by many workers for this purpose. Application of the S.M. to nuclear thermometry has been pioneered by Wheatley and his group[5]. In this laboratory, such a set-up has been assembled and tested by G. Lamarche, B. Hébral and the author, though not thoroughly exploited because of another development.

In the past, very low temperature nuclear magnetic thermometry has been realized through measurements of nuclear magnetic resonance signal amplitude and relaxation time τ_1. For this purpose two basic instruments have received the most attention. In the cw (continuous wave) method, marginal oscillator spectrometers were found to be adequate, giving mostly a signal amplitude response. A very elegant and powerful pulse method, the so called free precession technique, pioneered by Walstedt, Hahn, Froidevaux and Geissler[6] and further improved by them and other groups, where both signal amplitude and relaxation time measurements are obtained, permitted the realization of very good thermometers extending well into the sub mK range.

It is only recently that SQUID magentometers have been applied to the detection of N.M.R. Indeed, almost simultaneously Day[7] and Meredith, Picket and Symko[8] announced the first recordings of S.M.-N.M.R. spectra in adiabatic fast and slow passage respectively.

The new techniques appeared to be most promising both in terms of signal amplitude and relaxation time measurements for the low temperature thermometry application of S.M. and it was decided to concentrate our effort in developing them further. Outside thermometry, there appears to be, as well, some advantage in using S.M.-N.M.R., as it offers a very simple means of measuring the long relaxation times τ_1[9,10], usually encountered in insulating materials, especially at low temperatures.

This thesis is then a contribution to this new field of S.M.-N.M.R. and describes two investigations; one applies the technique of A.S.P. (adiabatic slow passage) on a metal sample at 4.2K as a first step in the construction of a nuclear thermometer, and the other makes use of the technique of A.F.P. (adiabatic fast passage) with a view to the possible exploitation of S.M.-N.M.R. in the study of relaxation times in insulators. As a result of this second investigation we have been able to study the variation of the relaxation time, τ_1, as a function of the applied field (3 - 30 mT) in a sample of CaF_2.

In what follows, we shall first discuss the SQUID with respect to the coupling of a signal to the device, N.M.R. and thermometry from the points of view of slow and fast passage, and finally the use of fast passage in the study of long relaxation times. This will constitute

Chapter I. Chapter II will deal with the experimental apparatus and the procedure for obtaining the N.M.R. signals. Chapters III and IV respectively, will deal with the investigations into A.S.P. on a sample of a Copper wire bundle at 4.2K in a field of approximately 30 mT and A.F.P. on a sample of CaF_2 in fields 3.0 - 30.0 mT also at 4.2K. In Chapter III, the behaviour of the N.M.R. signal height of Cu^{63} as a function of the r.f. field amplitude B_1, is reported and compared to theory. Chapter IV gives the results for the behaviour of τ_1 as a function of B_o for a CaF_2 crystal oriented with the (111) direction along B_o. This crystal contains an impurity, tentatively identified as Mn, in an unknown concentration. The concluding remarks and recommendations for improvement of the experiment and future work, form the basis of Chapter V.

CHAPTER I

SQUID

The theory and operation of a r.f. biased symmetric SQUID has been extensively covered in the literature, and as such will not be discussed here. An excellent review of the theory and uses of a SQUID can be found in O.V. Lounasma's recent book[11]. It will suffice to mention a few salient points on the coupling of a signal to the SQUID sensor.

Flux changes are transferred from the location of the sample to the SQUID sensor by means of a superconducting flux transformer (S.F.T.). The S.F.T. consists of a signal coil (self-inductance - L_{sg}) and a transformer coil (self-inductance - L_{tr}). The coils are wound of superconducting niobium wire and connected together by means of tightly twisted leads of the same material (self-inductance - $L_{\ell d}$ = 0.3 μH/meter[11]). The signal coil fits snugly in one hole of the SQUID sensor (Fig. 1), immersed in the liquid helium bath at 4.2K. The transformer

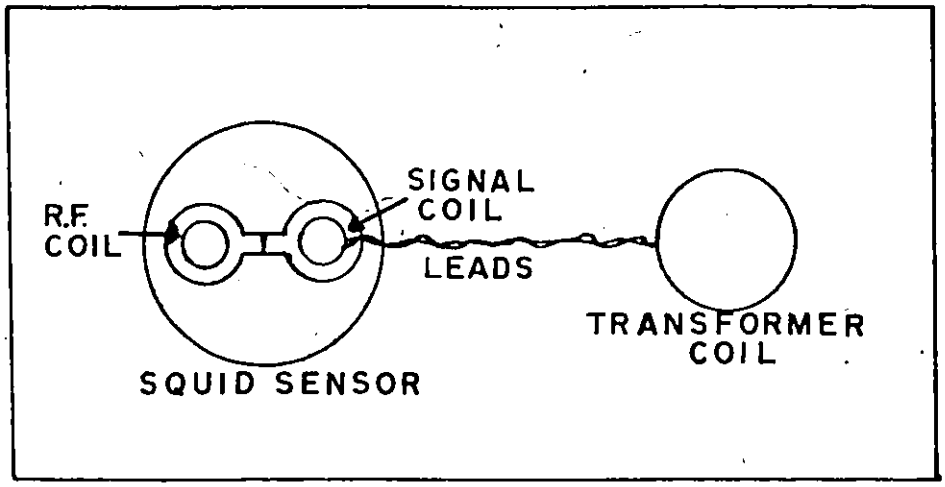

Figure 1. Schematic of superconducting flux transformer.

coil is either a single coil or a pair of astatically wound coils each of self-inductance $1/2\ L_{tr}$. In the first case, the coil is located around the sample and in the second only one of the two coils contains the sample.

Because the flux transformer consists of a bulk superconducting wire, the total magnetic flux, enclosed by the coils and the leads, remains constant at the value it had when the transformer was cooled through the superconducting transition temperature of the wire. When a change of flux, $\Delta\Phi_{ext}$, occurs at the transformer coil, a current J_{sg}, spontaneously begins to circulate along the superconducting wire to maintain a constant total flux. By definition, if the flux Φ, through each turn of a coil of N turns is the same, we may write

$$N\Phi = L_c J_c \tag{1}$$

where L_c is the self-inductance of the coil and J_c is the current flowing in it. Thus we find for a S.F.T.

$$N_{tr}\Delta\Phi_{ext} + (L_{tr} + L_{sg} + L_{\ell d})\, J_{sg} = 0 \tag{2}$$

where N_{tr} is the number of turns in the transformer coil. The amount of flux Φ_{sq} coupled to the sensor is

$$\Phi_{sq} = M_{sg}\, J_{sg} \tag{3}$$

where M_{sg} is the mutual inductance between the signal coil and the SQUID. Eliminating J_{sg} between (2) and (3) we obtain the basic equation for a

flux transformer

$$\Phi_{sq} = -\frac{M_{sg} N_{tr}}{(L_{tr} + L_{sg} + L_{\ell d})} \Phi_{ext} \qquad (4)$$

The quantity $M_{sg}N_{tr}/(L_{tr} + L_{sg} + L_{\ell d})$, is called the flux transfer factor and is generally considered to be maximized for $L_{tr} = L_{sg}$, providing (a) $L_{\ell d}$ is negligibly small with respect to $L_{tr} + L_{sg}$ and (b) that the coupling coefficient $K = M_{sg}^2/LL_{sg}$ (L is the self-inductance of the sensor) is kept constant. Typical values of the flux transfer factor range from 0.05 to 0.005.

The quantity Φ_{ext}, can be estimated by[12]

$$\Phi_{ext} = 4\pi\Delta M_o A_{eff} \qquad (5)$$

where A_{eff} is the effective area of the sample and ΔM_o is the change in magnetization. For a cylindrical sample that is long compared to the length of the transformer coil, we have $A_{eff} \simeq \pi d^2/4$, (the cross-sectional area). This effective area is actually the coil area multiplied by a filling factor. Thus the absolute value of the flux coupled to the SQUID is

$$\Phi_{sq} = \frac{4\pi M_{sq} N_{tr} \Delta M_o A_{eff}}{(L_{tr} + L_{sg} + L_{\ell d})} \qquad (6)$$

Having discussed the coupling of a signal to a SQUID, we will now examine the nature of this signal, as it applies to this work.

PRINCIPLE OF THE METHOD

The passage through nuclear magnetic resonance is detected by continuously monitoring the d.c. nuclear magnetization of a sample, placed in a constant magnetic field B_o, as the frequency of a r.f. field, at right angles to B_o, is swept through the Larmor frequency, ω_o.

In the work reported here, the sample was maintained at 4.2K. However, as we shall see shortly, the technique lends itself to thermometry and to the study of long relaxation times.

THEORY

At this juncture, it would be instructive to review some basics of nuclear paramagnetism with specific reference to the expected behaviour of the static magnetization with temperature.

From statistical thermodynamics we obtain for the magnetic part of the partition function z_B of a weakly interacting system of nuclear spins, the following expression[13]:

$$z_B = \sum_i \exp\left(\mu B\, m_i / kT_s\right) \tag{7}$$

Here μ is the magnitude of the nuclear magnetic moment, B is the polarizing magnetic field, k is Boltzman's constant, T_s is the spin temperature, and m_i is the magnetic quantum number.

For simplicity in notation, we will let

$$x \equiv \mu B/kT_s \tag{8}$$

Since m_i can take on the values -I, -I + 1, ... I-1, I, where I is the

magnitude of the nuclear spin, equation 4 may be written as

$$z_B = \sum_{m_i = -I}^{m_i = +I} e^{xm_i} = e^{-xI} + e^{-x(I-1)} \ldots e^{xI} \qquad (9)$$

Equation (9) is a finite geometric progression which can be simplified to obtain the following:

$$z_B = \frac{e^{-xI} - e^{x(I+1)}}{1 - e^{x}} \qquad (10)$$

Finally, on rearrangement of equation (10), the expression for the magnetic contribution to the partition function becomes

$$z_B = \frac{\sinh (I + 1/2)\, x}{\sinh 1/2\, x} \qquad (11)$$

The magnetization M of the spin system is given by

$$M = N k T_s \left(\frac{d \ln z_B}{dB} \right)_{T_s} \qquad (12)$$

where N is the number of spins.

On substitution of equation (11) into the above expression, we obtain for the nuclear magnetization

$$M = N \mu I B_I(x) \qquad (13)$$

where $B_I(s)$ is the Brillouin function and is defined as

$$B_I(x) \equiv (1 + \tfrac{1}{2I}) \coth (1 + \tfrac{1}{2I})\, x - \tfrac{1}{2I} \coth (\tfrac{1}{2I})x \qquad (14)$$

Of interest in this work, is the low field limit where $x << 1$. For this case, the hyperbolic cotangents of the Brillouin function

may be approximated by

$$\coth x = \frac{1}{x} + \frac{x}{3} - \frac{x^3}{45} \quad .... \tag{15}$$

Since x is very small, the first two terms of equation (15) are retained and when substituted into equation (14), the expression for the magnetization of an assembly of nuclei becomes

$$M = \frac{N\mu^2 I(I+1)B}{3kT_s} \tag{16}$$

This is Curie's equation for the magnetization of a paramagnetic substance and the Curie constant is thus defined as

$$C \equiv N\mu^2 I(I+1)/3k \tag{17}$$

Because of the weak internal interactions between the nuclei, the nuclear susceptibility χ_N would be expected to follow a 1/T behaviour well into the milli-kelvin range. In fact, it is estimated that for metallic copper, the nuclear spins would have an ordering temperature of approximately 10^{-7} K. Thus, the magnetic temperature T^*, obtained from a measure of χ_N would be equal to T, the absolute temperature, over a very wide range. Indeed, static magnetization measurements on very pure copper samples have shown the expected behaviour down to 10 mK[5,14]. Providing accurate measurements of χ_N can be made, the nuclear spin system is a convenient thermometer[15].

For a spin system to be useful as a thermometer, the characteristic time τ_1, that the nuclear spins take to come to equilibrium with the lattice at a temperature T should be short to insure rapid response to temperature changes, (or field changes). For this reason, only metals will be

considered for thermometric purposes as the relaxation times of insulators are much longer.

In metals the temperature dependence of the nuclear spin-lattice relaxation time τ_1 is given by Korringa's relation:

$$\tau_1 T = \beta \tag{18}$$

where T is the lattice temperature and β is Korringa's constant. For a metal such as copper, β is 1.3 sK. The relaxation time τ_1 is also field dependent[12] and for a field B, it is given by

$$\tau_1 (B) = \tau_1 \left[\frac{B^2 + b^2}{B^2 + 2b^2} \right] \tag{19}$$

Here b is the induction due to an effective internal field caused by dipolar or exchange interactions and τ_1 is the high field relaxation time. Further mention of τ_1 will be made later with regards to N.M.R. and the use of the Korringa constant to determine the temperature.

To measure the nuclear susceptibility, very sensitive instrumentation is required. As such, when static susceptibility measurements are performed, a problem arises due to contributions of an electronic origin to the magnetization. Since it is useful to work at low fields to reduce the relaxation time, the electronic background due to these impurities may not be saturated and thus could be a great nuisance until ordering of the impurity electronic spin system occurs. Nuclear magnetic resonance provides the answer to the problem, in that the magnetization measured is that of the nuclei only. However, fields of the order of 100 gauss are required, so that the relaxation times

encountered will be essentially the 'high field' relaxation times.

Let us consider a system of nuclei in a static magnetic field, B_{oz}. The system is irradiated along the x axis by a linearly polarized r.f. magnetic field given by

$$B_{r.f.} = 2B_1 \cos(\omega t)\hat{i} \tag{20}$$

Such a field can be considered as being composed of two fields of amplitude B_1, rotating in the xy plane in opposite directions, with angular velocities $\pm \omega$. Thus, the r.f. field of interest is that component of $B_{r.f.}$ which is rotating in the same sense as the Larmor frequency, ω_o.

When the frequency ω of B_1 is swept at a constant rate $S = d\omega/dt$ through resonance, the nuclear spin system absorbs energy from the r.f. field, causing the energy level population distribution to change. The rate S determines whether this is a slow or fast passage method.

In a slow passage, the rate at which the frequency is swept must be such that the time taken to pass through the resonance line is much greater than τ_1 . Thus if $\Delta\omega_{1/2}$ is the line width (due to dipolar interactions etc.) of the sample, then slow passage requires that

$$\Delta\omega_{1/2}/S > \tau_1 \tag{21}$$

If this condition is met, then at ω_o, the energy level population distribution will be such that M_z, the magnetization of the system in the z direction will have changed from M_{oz}, the value far from resonance to a value M_{1z} that will be determined by the amplitude of the r.f.

field. This dependence on B_1 will be discussed shortly.

In fast passage, the time spent passing through resonance is much less than τ_1. Under this condition, the magentization M_z immediately after sweeping through $2\Delta\omega_{1/2}$ is equal to $-M_{oz}$. In other words, the energy level population distribution has been reversed.

Consider for a moment a free spin situated in an effective field[16]

$$B_e = \left[B_o + \omega/\gamma\right] \hat{k} + B_1 \hat{i} \qquad (22)$$

This field is static in a frame of reference, rotating such that the motion of the spin's magnetic moment is a Larmor precession about B_e of angular velocity $\delta = -\gamma B_e$. By definition $B_o \hat{k} = -(\omega_o/\gamma)\, \hat{k}$, where γ is the gyromagnetic ratio. At resonance then, the effective field is equal to $B_1 \hat{i}$. The magnitude of B_1 fixes the upper limit of S, in that, for the magnetization to follow the effective field, the rate of change of frequency must be very much less than $\gamma^2 B_1^2$ i.e.

$$S \ll \gamma^2 B_1^2 \qquad (23)$$

The condition arises from the adiabatic theorem[16] which it must be stressed is derived for a free spin. From the preceding discussion of slow and fast passage, this limit will be of greater importance in the latter case. It must be noted, however, that in a real system of weakly interacting spins this condition should be strictly adhered to for the fast passage to be adiabatic. If not, as the rate S becomes of the order of $(\gamma B_1)^2$ there will be a corresponding loss of signal height owing

to the fact that an ever increasing fraction of the spins do not interact long enough with the r.f. field for there to be a precession about the effective field. The effect of a very rapid rate is to cause a perturbation of the magnetization which will die down with a characteristic time τ_2 (the spin-spin interaction time). This is not a reversal of population but a mere tipping of the magnetization.

The lower limit of S for fast passage is controlled by the greatest of the three following fields, B_1, B_L, ΔB; where B_L is the local field due to interactions between spins, and ΔB is the inhomogeneity of the applied field. Thus the conditions for fast passage in a solid are[16]

$$\gamma^2 B_1^2 \gg S \gg \max\left(\frac{\gamma B_1}{\tau_1}, \frac{\gamma B_L}{\tau_1}, \frac{\gamma \Delta B}{\tau_1}\right) \qquad (24)$$

If the z component of magnetization is monitored instead of the transverse magnetization, as is customary in N.M.R. techniques, then the further condition that $\frac{1}{T_2} \approx \gamma B_1$, is not applicable. In conventional N.M.R., the signal due to the detection of the transverse magnetization is reduced in the ratio B_1/B_L[16]. E.P. Day[7] has reported maximum signals for lines 0.8 mT wide using r.f. amplitudes of approximately 5.0 μT when monitoring M_z.

In slow passage, the magnetization is expected to follow the Block equations, which state that M_z will change from M_{oz} to a value M_{1z} at ω_o, given by[16]

$$M_{1z} = \frac{M_{oz}}{1 + \gamma^2 B_1^2 \tau_1 \tau_2} \qquad (25)$$

Here M_{oz} is the magnetization far from resonance and τ_2 is the spin-spin interaction time.

Since in this work we are interested in ΔM_z, the amplitude h_{sp} of the observed resonance line is proportional to $M_{oz} - M_{1z}$

$$h_{sp} \alpha \frac{M_{oz}\gamma^2 B_1^2 \tau_1 \tau_2}{1 + \gamma^2 B_1^2 \tau_1 \tau_2} \tag{26}$$

In writing equations (25) and (26), we have assumed that the whole sample is irradiated by a uniform r.f. field. This however is usually not the case and as such the symbol W will be substituted for and assumed to be proportional to $\gamma^2 B_1^2$. Thus equation (26) becomes

$$h_{sp} \alpha \frac{M_{oz} W \tau_1 \tau_2}{(1 + W \tau_1 \tau_2)} \tag{27}$$

If the sample is a metal, then τ_1 can be replaced by the Korringa relation (equation (18)). Also, as demonstrated by equation (16), the magnetization is proportional to B/T_s. Thus incorporating both factors into equation (27), we obtain an expression for the amplitude of the slow passage resonance signal as a function of temperature.

$$h_{sp} \alpha \frac{W\beta \tau_2 B_{oz}}{T(T + W\beta \tau_2)} \tag{28}$$

as indicated by Meredith et al[17], for a given value of B_{oz}, the amplitude h, will vary as T^{-2} for low power and as T^{-1} for high power.

Since it is relatively difficult to obtain very pure metal powders, the sample studied usually consists of a bundle of fine wires (5×10^{-5} to 10^{-5} m in diameter). The small diameter is to insure penetration of the r.f. field into the sample. The eddy current heating per unit volume, for a cylindrical conductor of radius R and resistivity ρ,

irradiated by a r.f. field of amplitude B_1, (assuming full field penetration) is[15]

$$Q = \frac{\pi^2 R^2 f^2 B_1^2}{16\rho} \qquad (29)$$

This heating is usually much greater than that due to the power absorbed by the spins at resonance. Thus, especially at low temperatures (mK range) it is important that the amplitude of B_1 be kept small in order that the temperature of the lattice is not unduly affected. The eddy current heating in a bundle of copper wires (5900 wires 2.5×10^{-5} meters radius, 6.4×10^{-3} meters in length) in a field B_0 of 30 mT and alternating field B_1 of 2 μT amplitude, at resonance is 6.8×10^{-8} Watts at 4.2 K. At 10 mK, the expected N.M.R. signal from the Cu^{63} spin system, calculated from (26) would be 660 times greater than the signal at 4.2 K. If now, the amplitude of B_1 is reduced to 0.1 μT, the expected signal at 10 mK would be 427 times greater than the signal at 4.2K for B_1 = 2 μT. This is still a very large signal, but the eddy current heating is reduced by a factor of 400. Even this amount of heat, however, will cause problems in the mK range, especially since slow passage requires the time taken to pass through resonance to be greater than τ_1 (21).

Using a fast passage regime, the sweep times are reduced, and thus there is less eddy current heating of the sample. Fast passage is essentially a 180^0 pulse which implies that the spin system will be at a temperature of $-T_s$ after the pulse. Thus, if the r.f. field is removed at the end of the sweep, the spin system should decay back to equilibrium with the lattice, in a time given by Korringa's relation. Therefore, fast passage gives two ways of measuring the temperature; the relaxation time combined with the known Korringa constant, and the

signal height h_{fp} which is proportional to $2M_{0z}$.

It must be stressed, that for the signal height to be used for thermometry the condition for adiabaticity must be stringently obeyed. As we have seen, the lower the temperature, the longer is the relaxation time in a metal. Thus the right hand condition of equation (24) is easily met. However, as mentioned in the discussion on eddy current heating, it is advantageous to reduce B_1 at low temperatures. If B_1 is reduced, care must be taken to insure that the left hand condition of (24) is also met. If not, the fast passage will not be adiabatic and the signal height will not be proportional to $2M_{0z}$. Thus, there is a limit to how low B_1 may be reduced and still maintain adiabaticity. For example, consider B_1 = 0.1 μT, and a copper sample. We will take as the maximum field of the right hand condition of equation (24), B_L, which for Cu^{63} is 0.3 mT. Under these conditions we obtain for the "limits" of the sweep rate at T = .001 K

$$50.3 \gg S \gg .017$$

It would obviously be difficult to satisfy the condition for adiabaticity and still have a reasonably low heat influx due to eddy current heating. Thus it can be seen that this type of thermometer would have a limited lower range.

In the temperature range where the fast passage thermometer would be useful, the signal maximum will follow a simple 1/T behaviour rather than the more complicated behaviour of the slow passage signal.

If we assume that the constant of proportionality is the same for slow and fast passage, then the signal height maxima can be compared. The ratio of h_{fp} to h_{sp} indicates that at a given temperature the fast passage signal will be greater than the slow passage by a factor of $\frac{2(1 + \gamma^2 B_1^2 \tau_1 \tau_2)}{\gamma^2 B_1^2 \tau_1 \tau_2}$.

It will be possible then to use fast passage to study relaxation in spin systems and obtain reasonably accurate values of τ_1 with or without the presence of an r.f. field, after reversal has occurred, as the signals will be large and as such easy to work with (good signal to noise ratio). The magnetization M_z, should follow an exponential decay according to

$$M_z = M_o \left[1 - 2\exp(-t/\tau_1) \right] \tag{30}$$

Thus as the SQUID signal will follow M_z, a plot of $\ln h_{fp}$ vs time will yield τ_1.

Meredith et al[17] have compared the signal-to-noise ratios for S.M.-N.M.R. and a conventional detection system. Under the optimum conditions for each method of detection we have

$$\frac{(\Phi_s/\Phi_N)_{max}}{(\nu_s/\nu_N)_{max}} = \frac{240}{\omega_o^{1/2}} \left(\frac{\tau_1}{\tau_2} \right)^{1/2} \tag{31}$$

The ratio of sensitivities are equal at a frequency given by

$$\nu_o = 10^4 \tau_1/\tau_2 \tag{32}$$

The advantage of N.M.R. detection by a SQUID magnetometer is obviously at low resonance frequencies and long relaxation times.

CHAPTER II

INTRODUCTION

In this Chapter we will deal with various aspects of the components that comprise the total experimental set-up, ranging from a general description, to the effects these components have on the experiments, vis-a-vis noise (mechanical and electrical) signal size, and liquid helium consumption.

Each component, that was constructed for this work, will be mentioned separately. All electronics, including the SQUID, will be dealt within one section. Finally, to conclude the Chapter, the manner in which the components fit together to form the experimental set-up will be discussed along with the general procedure.

ELECTRONIC APPARATUS

This section will deal with the main items of equipment that were utilized in these experiments. We will discuss briefly the experimental set-up of this equipment and then examine each individual component afterwards.

Fig. (2) is a block diagram of the experimental electronic set-up. Not shown in the figure, are the power supplies for the N.M.R. magnet and the manganin heater on the niobium field trap. Both the magnet and the field trap will be discussed later in this Chapter. Standard coaxial cables (RG-62/μ) with amphenol connectors were used to interconnect the various pieces of equipment. Matching cables were used to connect the digital voltmeter, the X-Y recorder and the oscilloscope to the SQUID electronics.

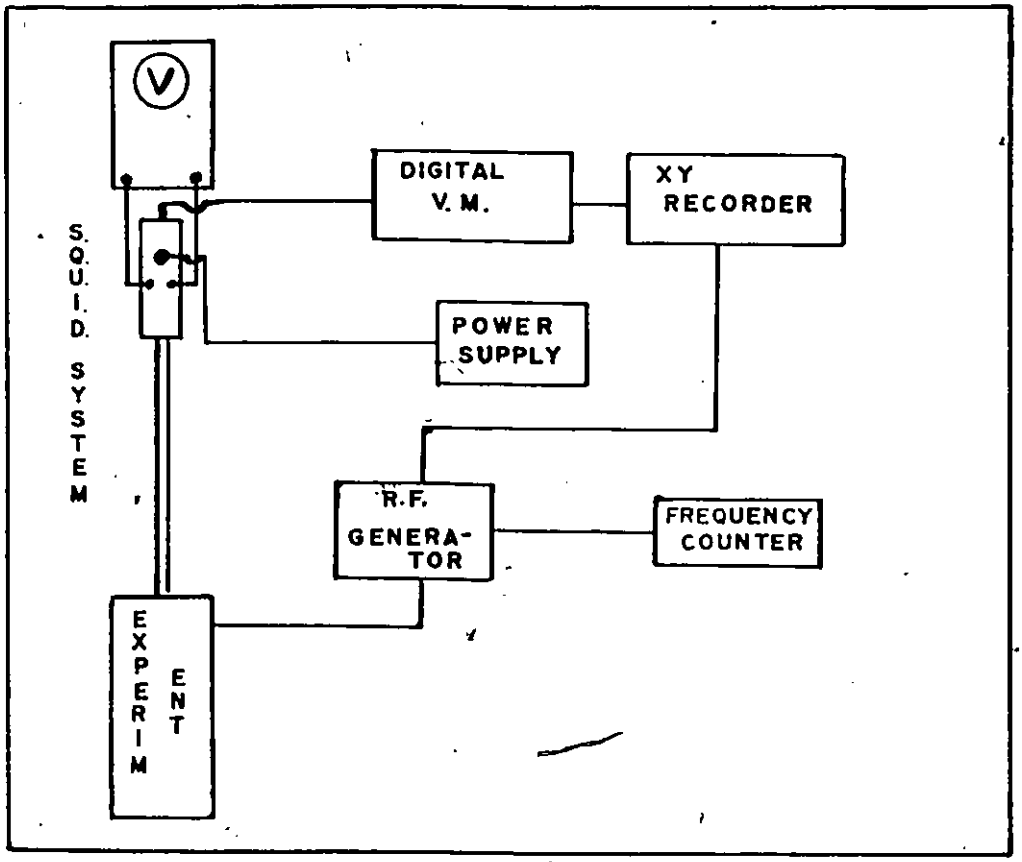

Figure 2. Block diagram of electronic experimental set-up.

The power for all the electrical equipment was supplied from a panel of eighteen grounded outlets, wired in parallel and connected to an independent twenty amp, 110 volt circuit in the laboratory.

Each side of the incoming power line, was connected to the line ground through a 0.1 microfarad 1000 v capacitor. Thus any transients on the line would be shunted to ground through the capacitors which also maintain the ground at zero potential, with respect to the line at all time.

Previous to the use of this panel, sixty cycle pickup was a considerable problem. The Tektronix 504 oscilloscope monitoring the lock-on mode of the SQUID electronics (to be discussed later in this Chapter) would display multiple patterns on the screen. This pickup, superimposed on the d.c. signal output of the SQUID electronics, could easily be followed by the X-Y recorder. This increased the noise level and also resulted in the SQUID system being more susceptible to transient disturbances.

The system used in these experiments was a Model 202 'Superconducting Quantum Electronic System' (S.H.E.)[1a], which consisted of a r.f. biased symmetric niobium SQUID, a probe, to house the SQUID and link it to the SQUID electronics. The biasing frequency of this device was 19MHz. The single-point-contact is made between two 000-120 screws, one flattened at the tip and the other honed to a 90^{o} point. The contact is made in the center of the slit interconnecting the two holes as indicated in Fig. (3).

The adjusting screws, though obtainable from S.H.E., were manufactured in-house from unannealed niobium rod. Before installation, they were cleansed in acetone and then heated on a hot-plate until oxidized to a gold-brown colour. The point contact, once properly adjusted, will remain so unless the SQUID experiences a severe shock (mechanical, thermal or electrical i.e. a static discharge near the point-contact).

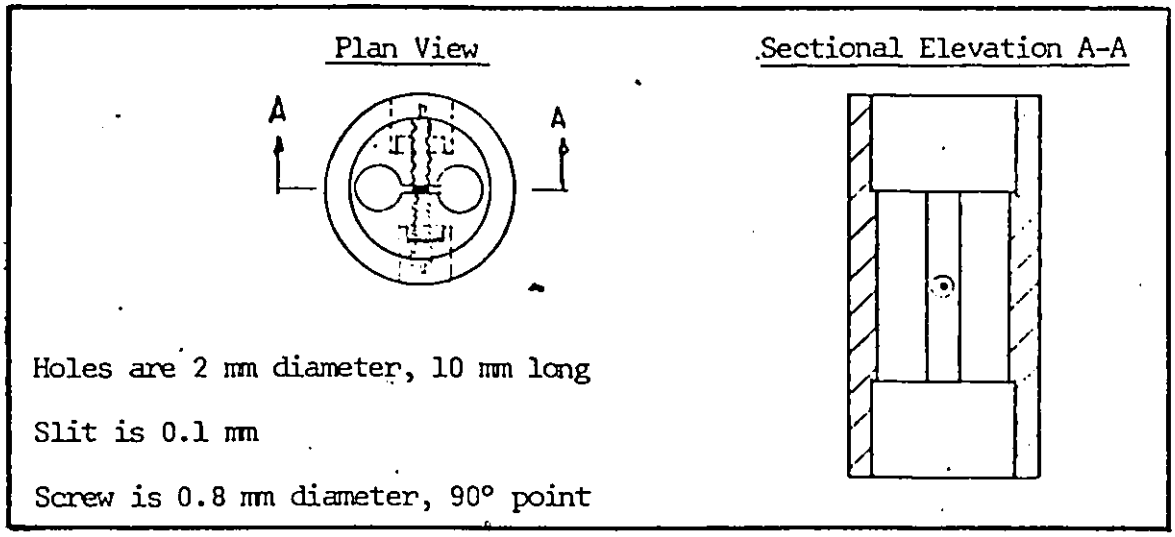

Figure 3. SQUID Sensor.

The SQUID system can be operated in one of three modes, the r.f. mode, the audio mode, and finally for the purpose of experimentation, the lock-on mode.

The r.f. mode, as illustrated in Fig. (4), produces a staircase pattern on the oscilloscope. This mode is used primarily for setting up and tuning the system. It is useful to turn on the electronics when cooling from 77K to 4.2K, as observation of the r.f. pattern as the SQUID cools through its superconducting transition temperature (9.2K), will indicate the condition of the point contact. If the contact is too weak, then the steps will be very noisy or missing altogether. If on the other hand, the contact is too strong, as transition occurs, the steps

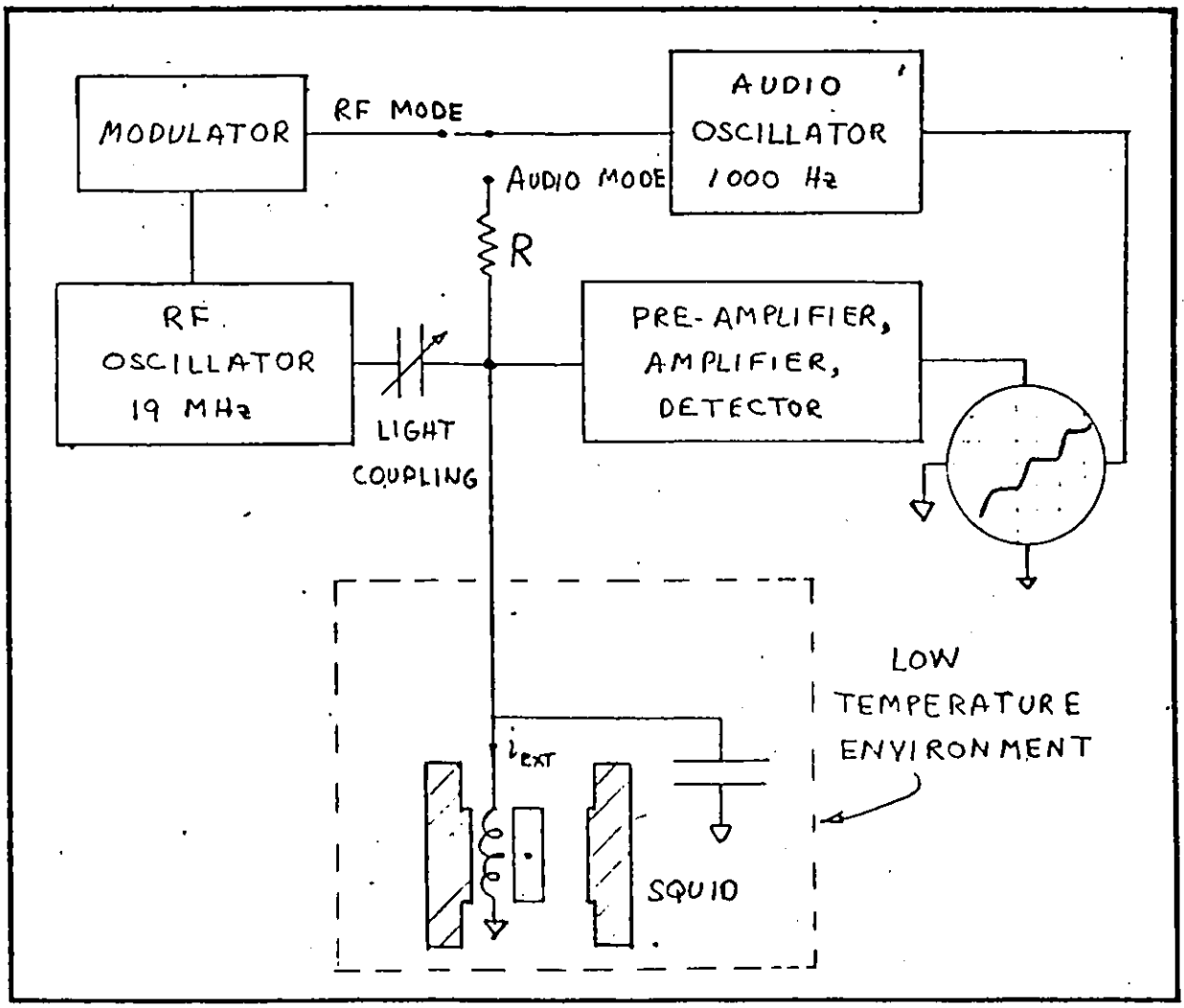

Figure 4. Block diagram of SQUID electronics circuit.

will be observed to travel up the display and disappear. In either event, the point contact must be re-adjusted.

If the system is functioning properly, then the electronics can be switched over to the audio mode. Slight adjustments of the r.f. level and the tuning capacitor are now required to maximize the amplitude of the triangular wave pattern displayed on the oscilloscope. This amplitude is approximately 50 mv for a well-adjusted system. Changes of flux, detected by the SQUID, will cause the triangular pattern to move across the oscilloscope. The displacement of one complete triangle is equivalent to the detection of a change of flux in the signal coil of the S.F.T. of one Φ_0.

When in the lock-on mode, as illustrated in Fig. (5), the oscilloscope display is a vee shaped pattern. For the particular system used here, this vee is distorted, in that there is an open loop on the right hand side and a spike in the center. The area of the loop is a function of the input level and is maximum for the highest setting of the ten-turn potentiometer (Fig. (6C)) controlling the level.

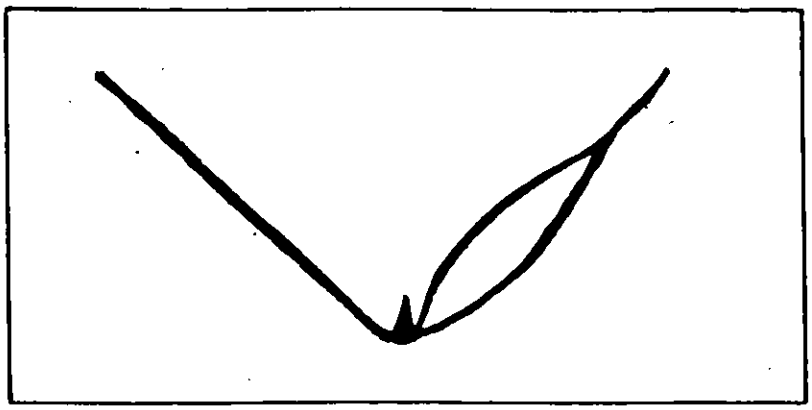

Figure 5. Lock-on mode display.

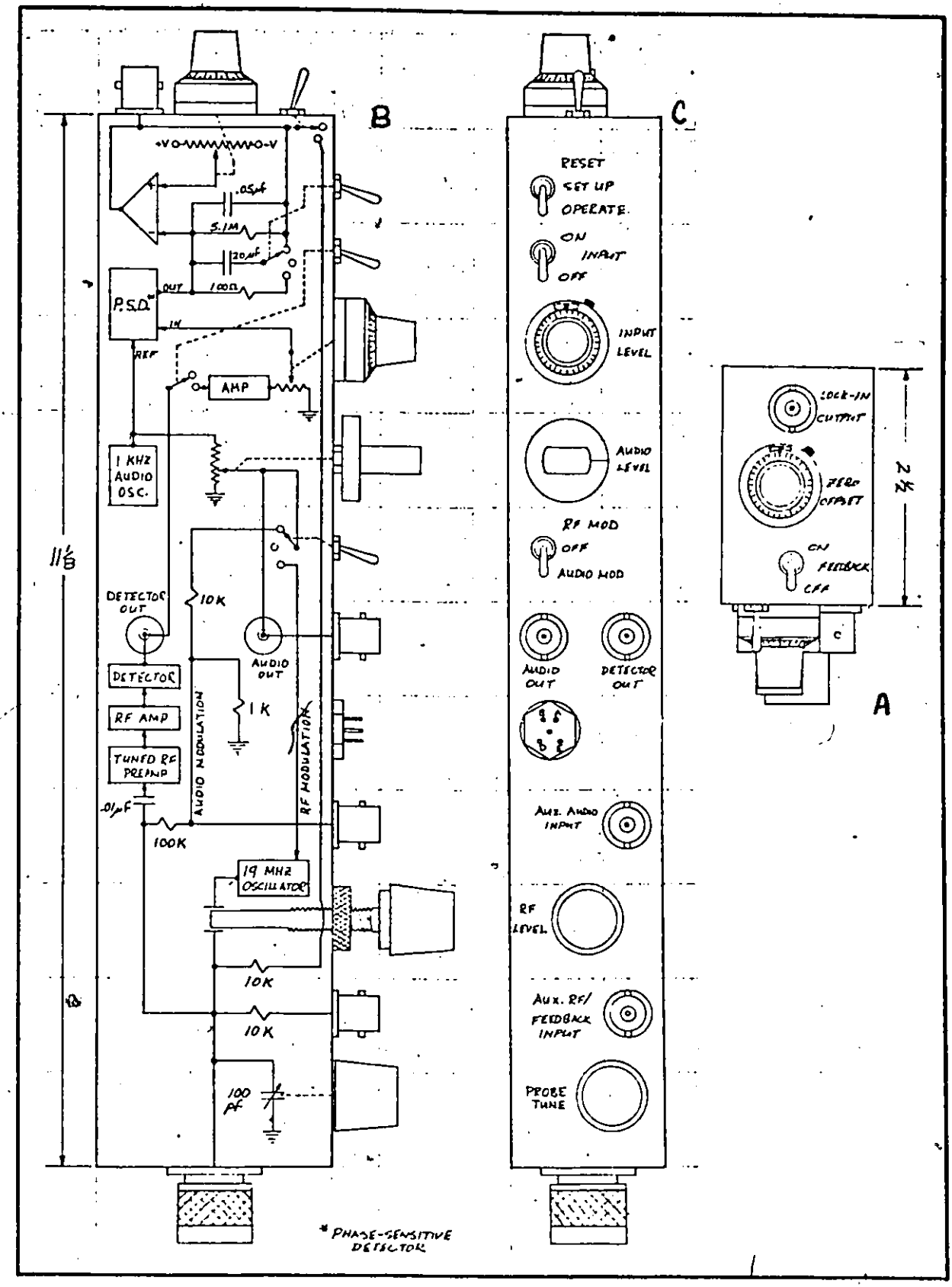

Figure 6. Model 202 SQUID Electronics.

The origin of the distortion is unknown at present.

When in the lock-on mode, the output of the lock-in amplifier is connected, through a 10 kΩ resistor, to the r.f. coil within one hole of the SQUID. The polarity of the feedback current is such that the r.f. coil produces a flux change equivalent but opposite in sign to that produced in the SQUID by the signal coil. Thus the total change of flux in the SQUID is zero. The feedback current is monitored by measuring the voltage drop across the 10 kΩ resistor. This voltage, measured at the lock-in output connector (Fig. (6A)) is therefore a linear function of the flux changes produced by the signal coil.

To measure the output voltage corresponding to one quantum of flux, the input switch (Fig. (6C)) is placed in the off position. The zero offset potentiometer (Fig. (6A)) is adjusted from its balance point, until the triangles sweep slowly across the oscilloscope screen. The detector output (Fig. (6C)) is used to drive the Y axis of an X-Y recorder. This output voltage oscillates at a frequency corresponding to the rate at which the triangles are drifting. The X axis is driven by the voltage from the lock-in output. The recorded result is a succession of triangles. Knowing the sensitivity of the X axis and the distance between a number of peaks, the voltage change per Φ_0 can easily be determined. For the system used in this work, the voltage Φ_0 was found to be typically (19.55 ± 0.03) mv.

Generally, the performance of this particular SQUID system was quite dependable. However, there were two problems of a sporadic nature, that presented considerable difficulty on occasion: (a) the noise level was unacceptably high and (b) the system sometimes became unstable

and measurements could not be made.

The noise had the form of an oscillation with a frequency centered at about six Hz. The amplitude of the distrubance was typically one mv.

The second problem appeared to originate from a bad point-contact. The step pattern of the r.f. mode was extremely noisy. As a result, the lock-in output voltage fluctuated greatly.

Both problems disappeared on cycling through transition and in no manner, whatsoever, could they be deliberately duplicated. One possibility is that the occurrence of these problems depends on the cooling rate from 77K to 4.2K. Perhaps, if the sensor is subjected to a mild thermal shock, stresses are created in the SQUID, which might either physically alter the point-contact or affect the superconducting currents flowing through it.

It is important that the voltmeter, utilized to monitor the lock-in output voltage, not generate transients at its input. Such transients would be injected back into the SQUID electronics via the lock-in output, and would pass directly through the 10KΩ resistor into the r.f. coil within the SQUID. This would result in a very unstable system and the lock-on mode would not function properly. The DANA 5330, (input resistance of 1000 meghoms for the 100 mv range) is relatively free from such transients. This instrument has two added features which were found to be very useful. The incoming signal is connected to a proportional analogue output of range 0-12 volts. Also, a single pole filter is available in the circuitry at the input, to reduce any noise of a sixty Hz origin.

The output voltage from the SQUID electronics was registered on 25 x 38 centimeter graph paper using an H.P. 7004B X-Y recorder. Both axes spanned a range of 0.25 mv/cm to 5 volts/cm. The signal from the electronics was connected to the Y axis of the recorder, either directly or from the analogue output of the DANA. The latter case was the usual procedure as the noise level was reduced by the previously mentioned filter.

The radio-frequency current needed to drive the saddle coils (see section on Sample Holder), was provided by either a Waveteck 164 Function Generator or a Hewlett Packard 8698 R.F. Generator. The H.P. 8698 was used for the N.M.R. measurements on the copper wire bundle (Chapter III). As this unit was not available for the measurements on CaF_2 (Chapter IV) the Waveteck 164 was utilized.

For both units, the frequency could be swept either continuously or in a single passage, between pre-adjusted end points on a ramp of positive or negative slope. The duration of the sweep between end points could be varied internally from 0.1-120 seconds and 10μS-100 seconds, for the H.P. 8698 and the Waveteck 164 respectively. These ranges could be greatly extended by placing either unit on a continous wave mode at a desired frequency (usually the resonance frequency) and making use of the external frequency modulation inputs. If a continuous triangular wave, of fixed frequency, was connected to the F.M. input, the result was a linear sweep of the output frequency between end points determined by the voltage amplitude of the modulation. The overall frequency range for the H.P. 8698 was 0.1 to 110 MH and that of the Waveteck 164, 30 μHz - 30 MHz.

Frequency measurements were made by monitoring the synchronous output on either generator with a General Radio model 1192 counter with a seven digit display. The frequency counter was capable of measuring up to 32 MHz with maximum resolution of 0.1 Hz. In the work reported here, the counter was set up to have a resolution of 10 Hz due to a sampling time of 0.1 seconds.

The H.P. 8698 is a stable instrument providing a very clean sinusoidal output signal. The Waveteck 164, on the other hand, was found to be unstable and the signal was slightly distorted. The distortion on the signal was not critical as it was just visible on an oscilloscope. Of more concern was a small d.c. ramp in the output of the generator observed during a sweep. This ramp was readily detected by the S.M. as a change in the local magnetic field. The resulting signal from the SQUID electronics, was approximately 40 mv for the maximum power output of the generator and was proportional to the power level setting of the Waveteck. This problem was eliminated by placing a 0.4 μf (20 v) capacitor in series with the r.f. output, between the unit and the coil, thus preventing any transmission of the d.c. ramp.

Another problem with the Waveteck 164 is that it is not shielded as is the H.P. 8698 and thus there is a great deal of r.f. leakage. This leakage was picked up by various leads in the set-up resulting in a very unstable functioning of the SQUID system in the MHz region. The instability was quite probably caused by an interference between this pick up and the 1 KHz frequency, utilized as the reference signal for the P.S.D. of the SQUID electronics when in the lock-in mode.

The problem was reduced somewhat by shielding the wires entering the helium dewar. Recent experiments in our laboratory have indicated that the problem would be essentially eliminated by using stainless steel dewars instead of glass ones and would be a simpler solution than placing the Waveteck or the experiment in a Faraday cage.

Two power supplies were required for these experiments, one for the N.M.R. magnet and the other for the heater on the superconducting Nb field trap.

The current for the N.M.R. magnet was supplied by a Hewlett Packard, Harrison 6260 A, D.C. power supply. This instrument is capable of delivering 1000 watts (10 volts, 100 amps) and was found to be a very stable supply.

A Krohn Hite model UHR-220; high voltage power supply capable of 100 watts output (max 200 milliamps, 500 volts) was used to generate the current for the heater. The high voltage was required as the resistance of the heater was quite large i.e. 2,260 ohms. Both the field trap and the heater will be discussed shortly.

DEWAR HEAD

A set of nested glass dewars was utilized to minimize the usage of liquid helium. This set consisted of a standard nitrogen dewar, 4.6 cm I.D. by 82 cm in depth, and a "tail" dewar to contain the helium. This dewar, 77.4 cm in overall inside length, was divided into an upper section, 8.5 cm. I.D. by 40 cm, and a lower section, 2.5 cm I.D. by 37.4 cm.

The helium dewar was sealed as indicated in Fig. (7(i)). A tight fitting styrofoam plug, in which the stainless-steel tubes (0.5" OD) were embedded, extended 17 cm into the dewar, reducing the reservoir volume from 2.24 to 1.29 litres.

S.M. - N.M.R. HEAD

The magnetometer head was similar to those described previously by Day[7] and Meridith et al[16]. For the measurements on a sample of a copper wire bundle and a sample of CaF_2, the head was essentially the same as that depicted in Fig. (8).

Structurally, the head consisted of three main parts: (1) the field trap; (2) the radio-frequency shield; and (3) the sample holder.

(1) Field Trap

The field trap was a hollow cylinder machined from a 3/4" round bar of unannealed niobium. The overall length was 10.8 cm with an inner diameter of 1.67 cm and a wall thickness of 0.1 cm. The inside was thoroughly cleaned with acetone to remove all oil deposits from the machining. A bar of Araldite was then cast in the niobium cylinder. When cured, the cylinder was boared out leaving an Araldite sleeve of 0.1 cm thickness firmly adhered to the inner wall of the trap. This sleeve electrically insulated the radio-frequency shield from the field trap and permitted the trap to slide easily over the shield.

A 2200 ohm bifilar coil of #36 A.W.G. insulated manganin wire was wound on the outside of the trap with a 0.01" thick sheet of Mylar, insulating the coil from the trap. This Mylar was necessary as the wire

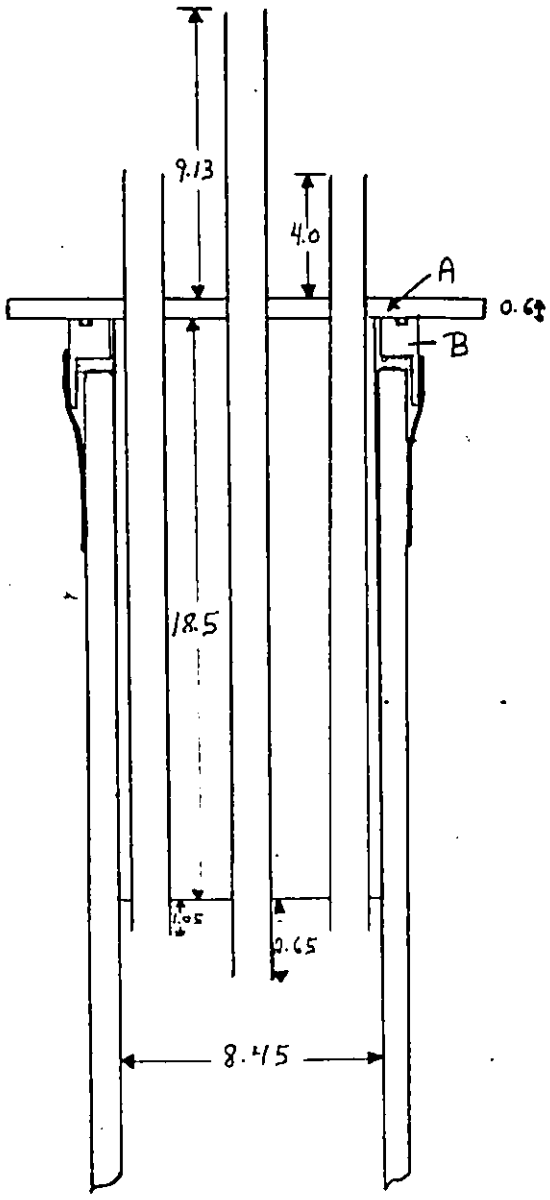

7(i)

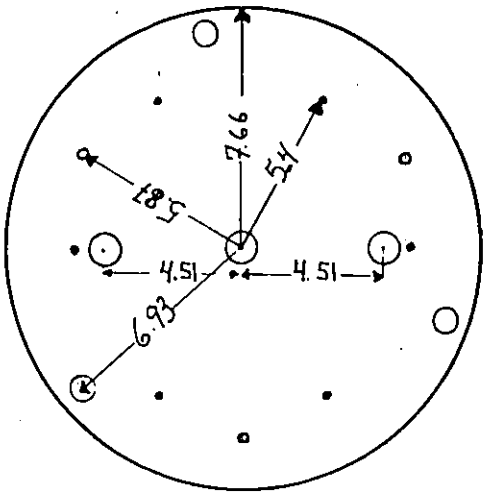

7(ii) Top view of A

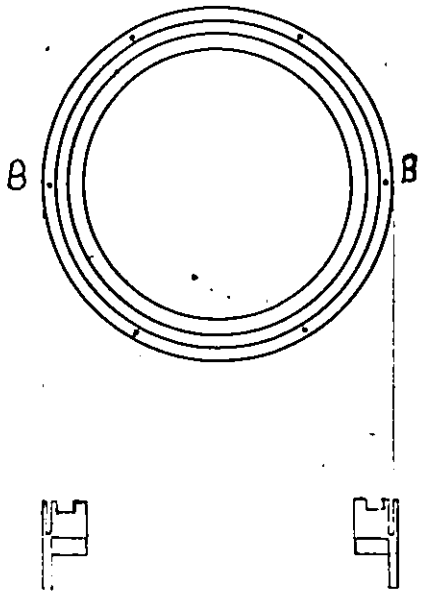

7(iii) Top & sectional view of B

Figure 7. Dewar Head.

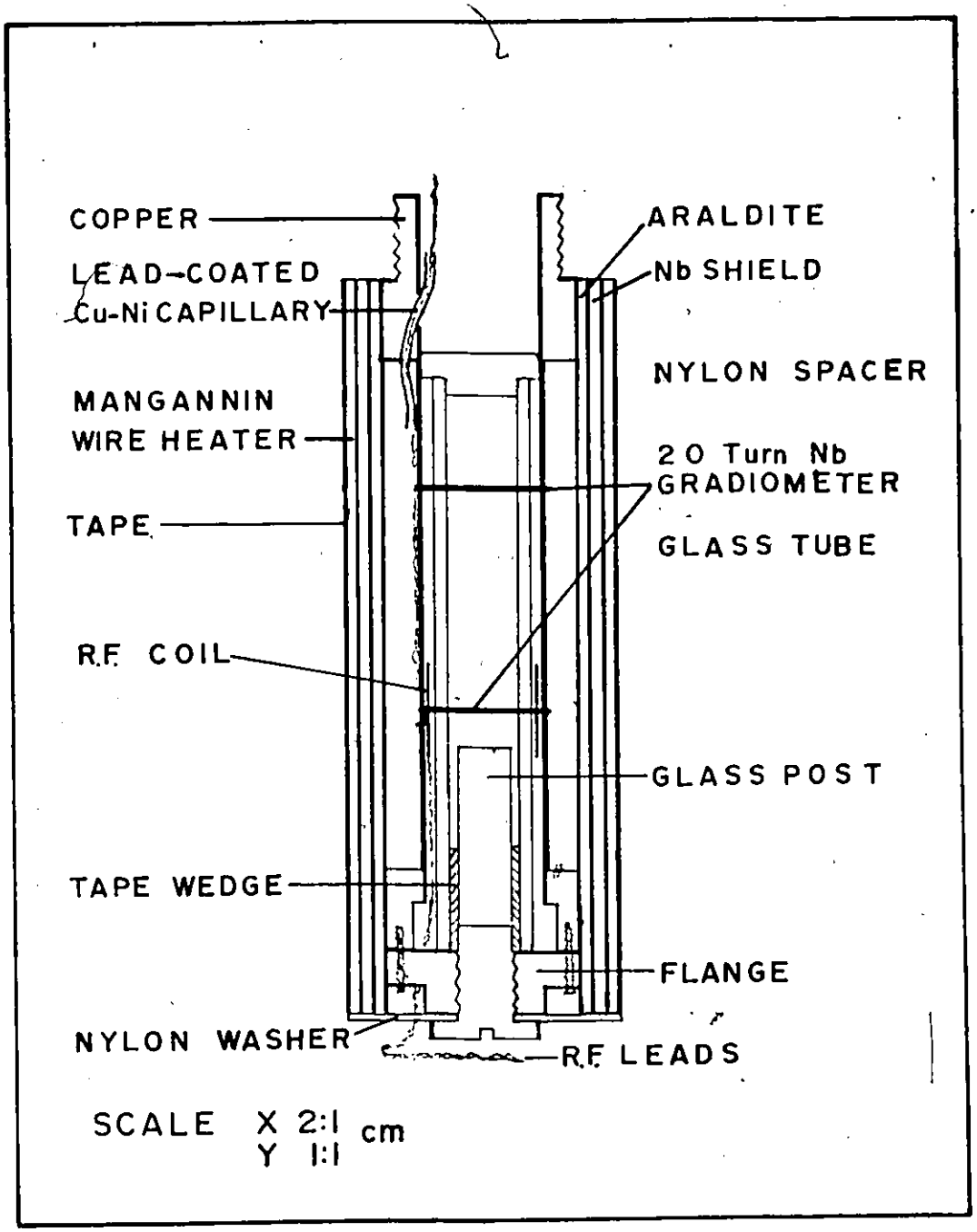

Figure 8. S.M. - N.M.R. Head.

insulation deteriorated on over-heating. The coil was used to drive the superconducting field trap normal permitting a new magnetic field to be trapped when the cylinder was cooled through the transition point (9.2K) in that field. To increase the efficiency of the heater, several layers of masking tape were wrapped on it, partially insulating the heater from the liquid helium.

(2) Radio Frequency Shield

The shield, machined from a round bar of copper stock, was 11.24 cm in length. Other dimensions, as well as the positioning of the shield were as indicated in Fig. (8). The 0.001" Mylar insulation covering the region where the gradiometer was wound, is not shown. The leads from the gradiometer were fed into an electrically insulated lead-coated copper-nickel capillary tube which passed through the shield into the region above the sample.

The gradiometer, part of the S.F.T., consisted of a pair of astatically wound coils of twenty turns of 0.003" insulated niobium wire. The inductance of the gradiometer was found to be 6×10^{-6} henries from the resonance frequency of an LCR circuit.

The coils were manually wound on the shield, electrically insulated by the Mylar sheet. However, since the coils were not wound on a former, slight geometrical variations resulted. This asymmetry would definitely produce an unbalanced gradiometer. Also it would have been advantageous to place an identical sample in the other coil of the gradiometer, to further equalize the inductances of both coils. Fortunately, this was not of great importance in this work.

The signal coil of the flux transformer was a fifty turn niobium wire coil wound in two layers. It was estimated that the mutual and self-inductances[12] of the coil, M_{sg} and L_{sg}, were 6×10^{-9} and 2×10^{-6} henries respectively. The twisted wire leads connecting the signal coil to the gradiometer were 10 cm in length. The estimated inductance was 0.3×10^{-7} henries. Thus, from equation (4) we obtain, $\Phi_{sq} = 0.015\ \Phi_{ext}$, where 0.015 is the flux transfer factor.

(3) Sample Holder

The sample holder was comprised of four parts; a thin walled tube, either of glass or delrin; a nylon screw and washer; and a copper flange.

The nylon screw was threaded into the copper flange with the washer held between the lead of the screw and the flange as indicated in Fig. (8). The diameter of the tip of the screw was the same as the inner diameter of the tube. The tube was thus held in position at the center of the shield by the tip of the screw and a nylon cap at the top of the tube. The flange was held firmly against the shield by four (00-90) screws threaded into the body of the shield. The washer supported the field trap, preventing it from slipping off the shield.

The r.f. coil used to induce the nuclear magnetic resonance was of the wrapped around saddle shape and was fastened on the sample tube by masking tape. The use of tape permitted easy demounting of the coil, enabling the tube to be cleansed.

The coil consisted of two identical rectangular coils, (10 turns #40 A.W.G. copper wire) wound such that each would enclose approximately 120^{o} of arc when taped to the tube. Typically, the assembled

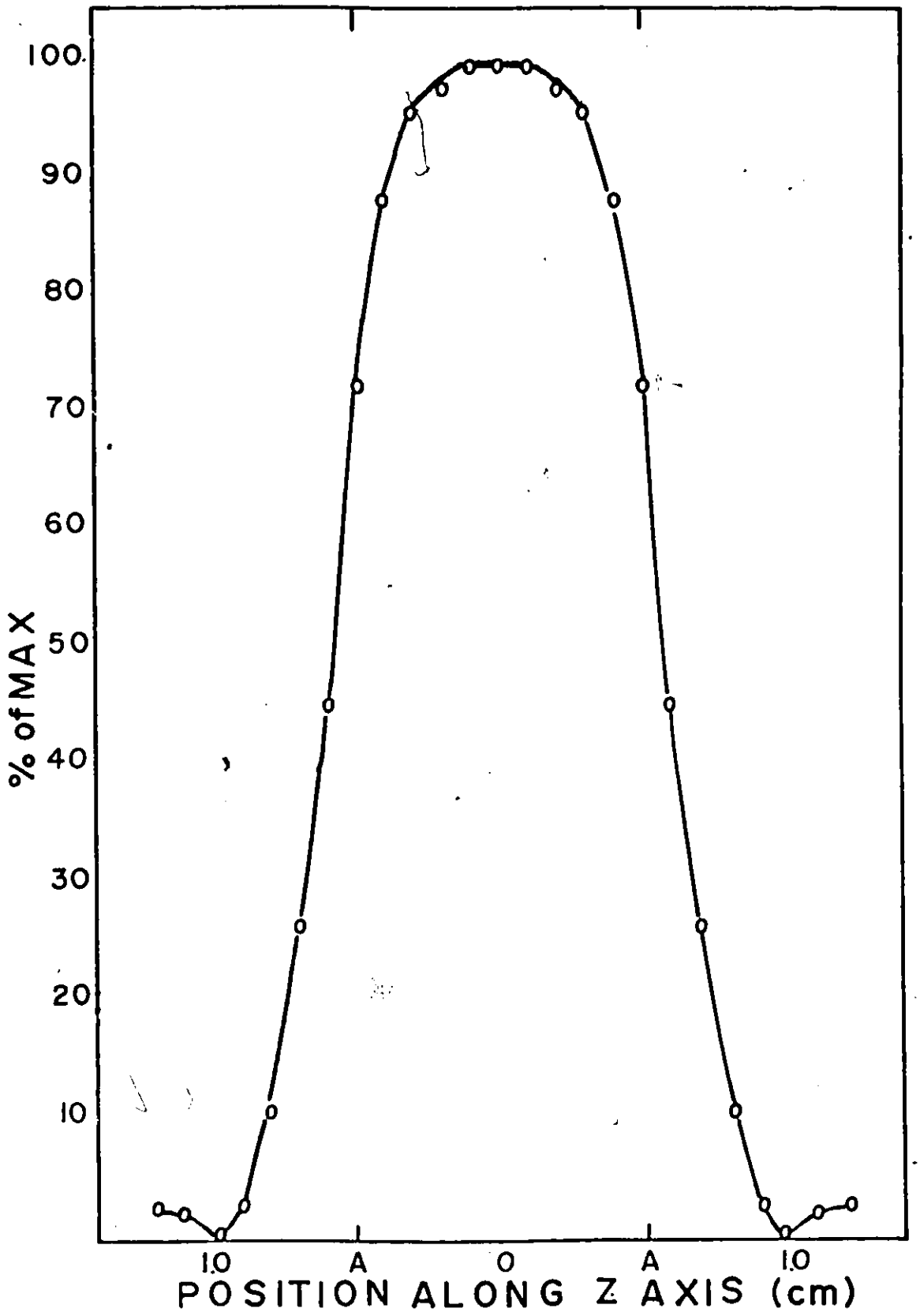

Graph (1). R.F. coil profile.

coil extended over a height of 1.4 cm.

The leads for the coil were passed through the copper flange in a teflon spaghetti (to insure electrical insulation) and soldered to the r.f. leads enclosed in a lead-coated Cu-Ni capillary tube taped to the outside of the field trap.

The profile of a typical coil was mapped, using a pick-up coil, of 0.03 cm^2 area, wound on a delrin former. The N.M.R. r.f. coil was driven at 1 MH_z at room temperature. The voltage induced in the pick-up coil was measured by a H.P. model 400H V.T.V.M. The profile is displayed in Graph (1). The section on the X axis marked A-A, was the region occupied by the CaF_2 sample (Chapter IV). The measured Q value of this particular coil was 40.

The field produced by a straight wire carrying a current I at a point P in the perpendicular plane which bisects the length (Fig. 9(a)) is[18]

$$B = \frac{\mu I}{4\pi R} (\sin\beta_1 + \sin\beta_2) \text{ Tesla} \qquad (32)$$

where μ is the magnetic permeability and R is the distance from the wire. Consider a group of four bundles of 10 wires 1.4 cm. in length, spaced as in Fig. (9b). The field at a point, equidistant from the bundles and in the previously mentioned perpendicular plane is $2B_1$ and thus we obtain

$$B_1 = 20B\cos\theta \qquad (33)$$

The angle θ for a perfectly wound coil is 30^{o}. Neglecting any possible contribution from the coil sections perpendicular to the bundles (Fig. (9 C)) (assumed to give zero field), the field factors for the empty saddle coils were 0.97 and 0.83 mT/amp, for the experiments on Copper and CaF_2, respectively.

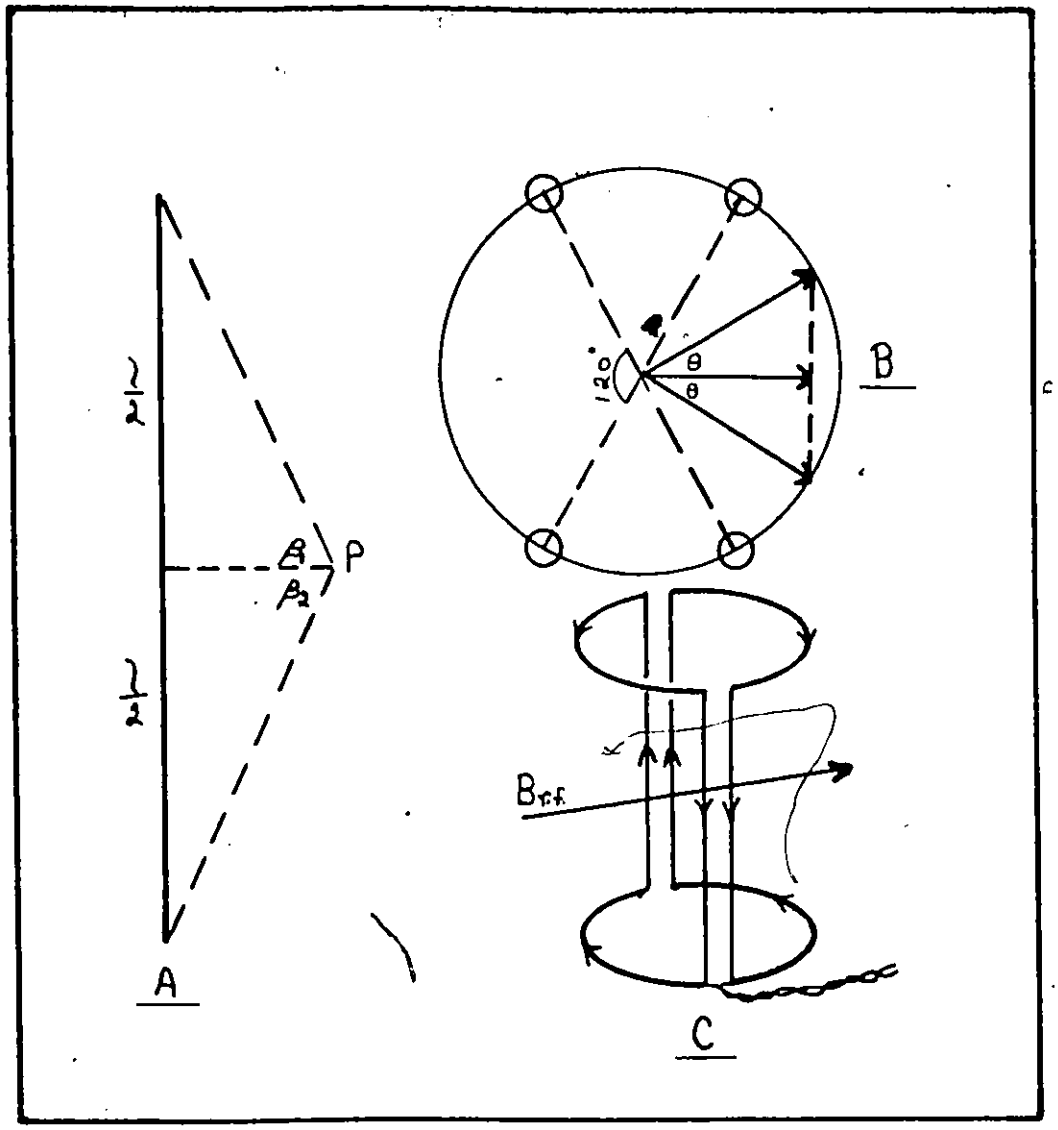

Figure 9. R.F. Coil.

N.M.R. MAGNET

The applied magnetic field for these experiments was produced by a simple liquid N_2 cooled copper wire wound solenoid, 15.3 cm in overall length. The solenoid was wound in four layers on a stainless-steel tube (I.D. 3.648 cm, O.D. 3.888 cm) with #18 A.W.G. copper wire. Each layer was separated from the preceding one by plastic strips (0.14 cm thick by 0.5 cm wide) placed parallel to the coil axis every centimeter about the circumference of the solenoid. The purpose of these strips was to create channels which would enable the liquid nitrogen to circulate freely between the layers. When immersed in liquid nitrogen, the resistance of the solenoid is .22 ohms. The Joule heating developed by this solenoid is $0.22\ i^2$ Watts.

The maximum current used in the work reported here was typically around 7 amps, corresponding to Joule heating of only 11 watts. This power output was quite readily dissipated in boiling the liquid nitrogen as the effective surface area of the solenoid, in direct contact with the liquid, was estimated to be 1200 cm^2.

The field at any point along the central axis of the solenoid can be calculated to a very good approximation using the following expression

$$B = \frac{\mu n I}{2} (\cos\theta_1 + \cos\theta_2) \qquad (34)$$

where $n = 3600$ is the number of turns per meter, I is the current measured in amps, and θ_1 and θ_2 are as indicated in Fig. (10) and B is the field expressed in Tesla.

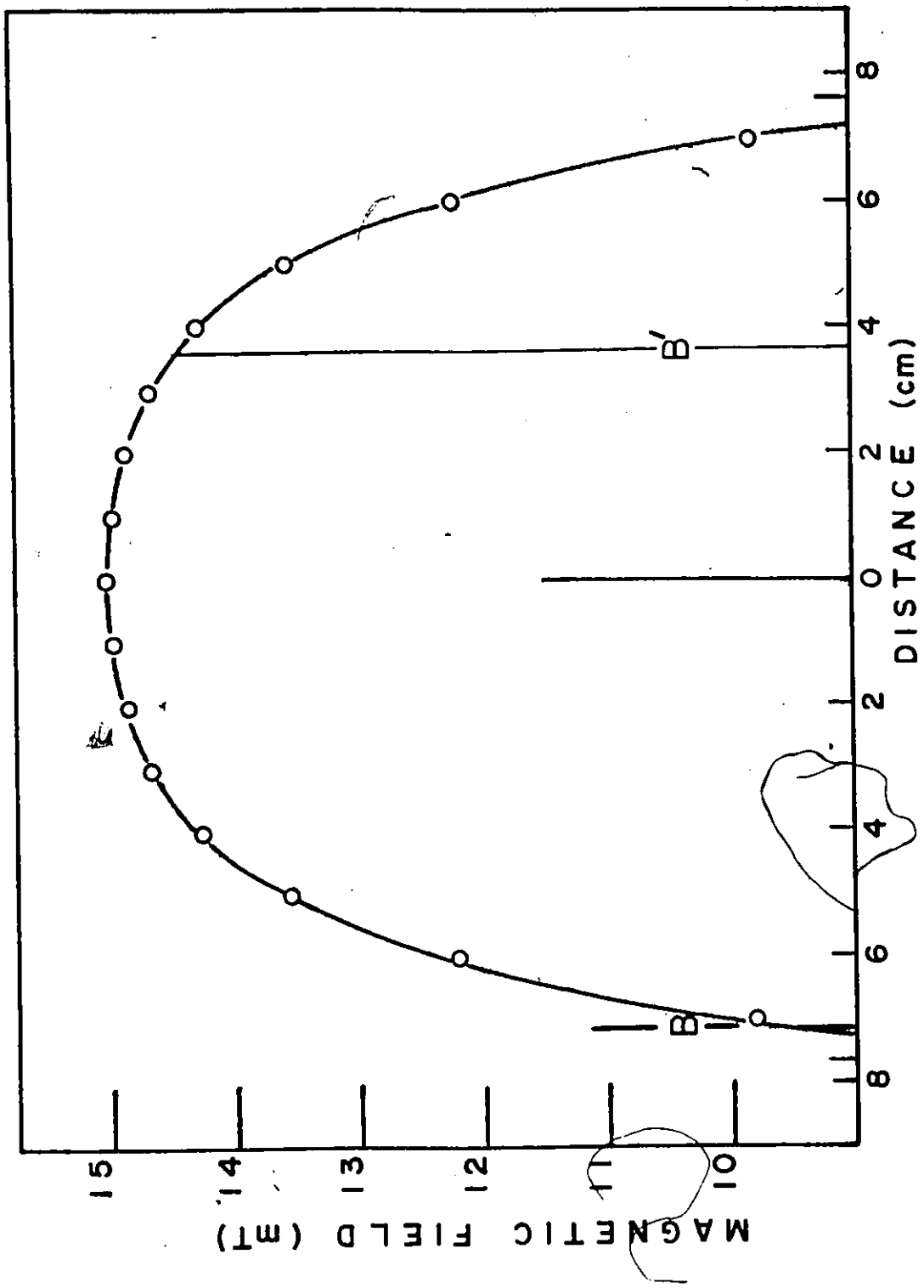

Graph (2). Calculated field profile of solenoid for center field of 15 mT.

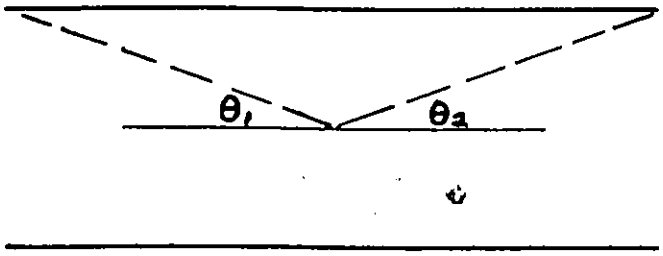

Figure 10.

The calculated field at the midpoint of the solenoid is 4.32 mT/amp. Graph (2) shows the field profile along the central axis for a midpoint field of 20 mT.

The points B and B' marked on the graph are the ends of the niobium field trap. If the niobium cylinder traps the field profile that it is situated in when cooled through transition, then, for a field of 20 mT, the lower end traps 12.6 mT and the upper end, 19.2mT. However, near the ends of the solenoid the above assumption is certainly not valid, as superconducting currents are induced due to the transition from superconducting to normal material. Thus, the fields measured at B and B' would in all likelyhood be quite different from those mentioned above. The actual field trapped at the sample site as infered from measurements will be discussed further in Chapters III and IV.

An inhomogeneity of the magnetic field will have at least one consequence and possibly a second. The first is that the line width of the N.M.R. signal, for both slow and fast passage, will be broadened. If the inhomogeneity is larger than B_1, the amplitude of the r.f. field, or B_L, the local field, then it will determine the lower limit of the condition for adiabatic fast passage as indicated in equation (24) of Chapter I.

ANTI-VIBRATION SYSTEM

Since the SQUID, the heart of the magnetometer, is extremely sensitive to changes in flux, any motion of the SQUID sensor and its input flux transformer will produce a background noise which could be large enough to obscure the N.M.R. signal. The maximum signal encountered in these experiments was 15 millivolts, which is of the order of the noise level to be expected from an improperly secured sensor. Thus, since most of the signals were smaller than that mentioned above (about 1 m.v. for Cu^{63}) it was imperative that this noise level be reduced.

The problem was attacked on two fronts: (1) the stray field at the site of the sensor was made as small as possible and (2) the S.M. to a great extent, was isolated from any source of vibration. The former shall be discussed in the next section.

The two main sources of vibration are the building and the boiling of liquid nitrogen and helium in their respective dewars. To dampen the vibrations from the building, the pair of nested glass dewars, in which the SQUID rod is centrally located, were attached to a plate floating on a combination of foam pads and a partially inflated rubber inner-tube. To lower the center of gravity and to decrease the natural frequency of the system, 25 Kg of lead was rigidly suspended 95 centimeters below the plate. The natural frequency was typically about 0.5 Hz, depending on the respective levels of the liquid nitrogen and liquid helium. Fig. (11) is a schematic diagram of this anti-vibration system.

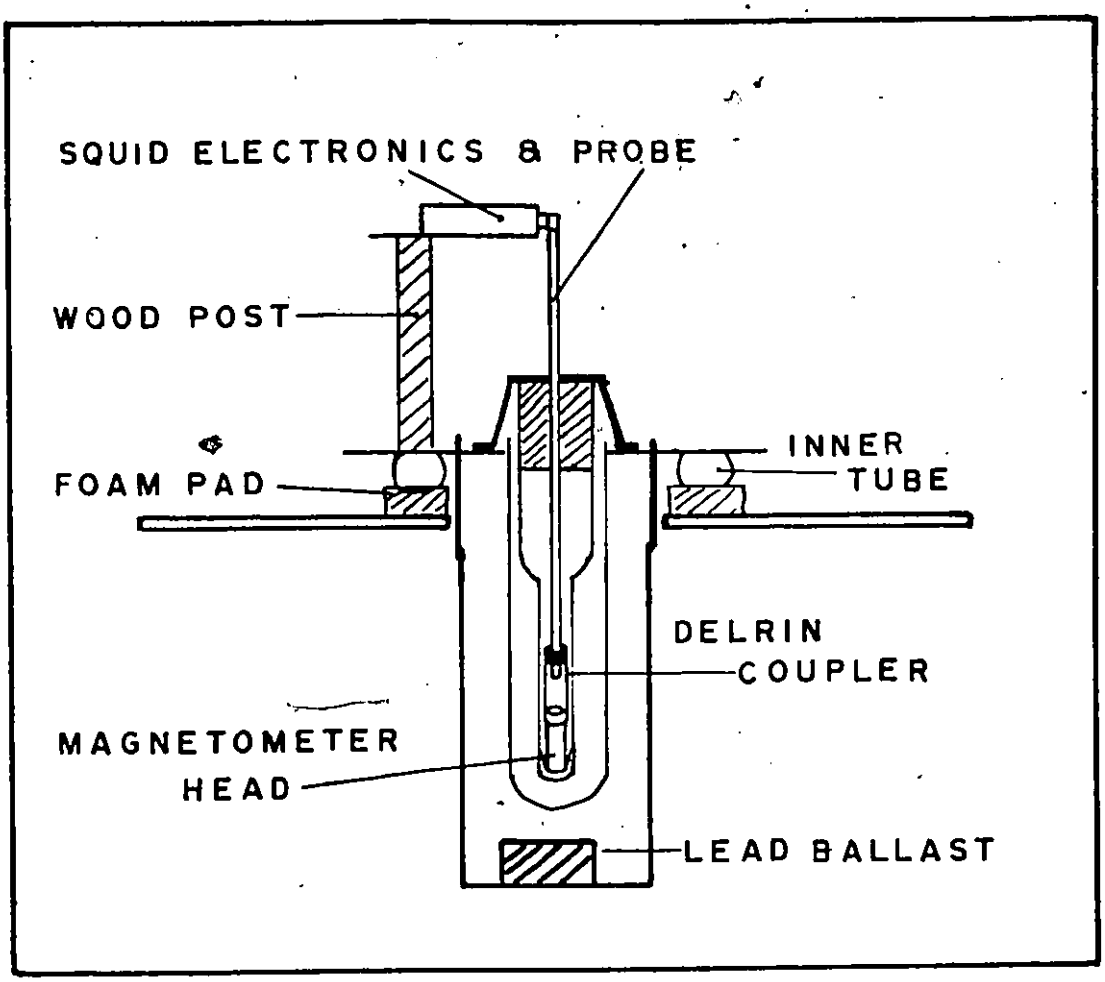

Figure 11. Anti-vibration system.

As indicated in Fig. (11) the magnetometer head was rigidly attached below the SQUID on the probe which was centrally located in the dewar. The probe was held rigidly at both ends of the central 1/2" stainless-steel tube (Fig. (7i)). The head screwed into the end of a delrin coupler which could be clamped onto the end of the probe. The nearest end of the field trap was 6 cm distant from the probe.

When attached, the probe and head constituted a rigid pendulum 54 cm in length. To dampen any motion of this pendulum six springs were taped, equally spaced about the circumference of the lower end of the magnetometer head. These springs were 5.0 x 0.5 cm strips of 0.015 cm thick beryllium-copper sheet, bent upwards at an angle of 45^{o} away from the head, about two thirds distant from the point where they were attached. The tip of the angled portion of each strip was in firm contact with the inner wall of the tail dewar, reducing the horizontal motion of the head, thus resulting in an acceptable noise level.

The amount of liquid helium used in an experiment was greatly reduced by the system previously described. Runs in stainless-steel dewars, typically consumed 10 litres of helium for similar experiments, whereas 3 litres of helium sufficed, in the glass dewars. However, this reduction of consumption was offset by the increased noise level introduced by the poor electromagnetic shielding afforded by the glass dewars.

Further, the anti-vibration system evolved for these experiments was probably not essential: this system grew out of investigations carried out previous to the N.M.R. studies. The original support for the dewars was, in hindsight, extremely unstable and was thus itself responsible for most of the mechanical noise.

Recent experiments in this laboratory conducted in stainless-steel dewars without using an anti-vibration mounting of any kind, showed similar or, even, better signal-to-noise ratios, than those obtained in the glass dewars.

PROCEDURE

Once the helium dewar was sealed, the vacuum jacket, which had previously been flushed with air to eliminate any trace of helium, was evacuated to a primary vacuum (≈50 microns). The dewar was then positioned on the plate (Figure 8) in the center of the liquid air dewar and connected to the helium return line.

While the liquid air dewar was being filled, the interior of the helium dewar was flushed for a few minutes with helium gas from a pressurized storage bottle to eliminate as much air as possible. Thus as the interior of the dewar cooled to liquid air temperature, helium gas could be drawn from the return line to maintain a constant positive pressure. The presence of a helium gas atmosphere was necessary as air would freeze out when liquid helium was transferred into the dewar, and should any air freeze on the point contact of the SQUID, damage to the contact would result.

Typically, the interior reached an equilibrium with the liquid air temperature in 4 hours. Prior to transferring, a final check was made of the electronic apparatus, the heater on the field trap and the N.M.R. radio-frequency coil.

Liquid helium was transferred into the dewar at a slow rate, typically 4 litres/hour, to insure that the SQUID would not be thermally shocked. Such a thermal shock would induce strains in the body of the symmetric SQUID which could damage the point contact.

Once the SQUID electronics package was adjusted to give the largest and cleanest triangle display on the oscilloscope, a d.c. voltage ramp was applied across the N.M.R. coil. Motion of the triangles

across the screen indicated that the flux transfer circuit was functioning properly. This test having been successfully concluded, the SQUID system was then placed in the "Lock-on" mode of operation.

To trap a magnetic field, the niobium cylinder was driven normal and then allowed to cool in the field of the N.M.R. magnet. The transition of the field trap from the superconducting to the normal state, was indicated by a momentary loss of "lock". The current flowing in the magnet and, hence, the field was determined from the voltage drop across a standard 5×10^{-4} ohm resistor.

A lead shield is positioned about the SQUID sensor and is firmly fastened to the probe. The shield becomes superconducting at about 7K, essentially trapping the Earth's field. If the stray magnetic field, typically 0.5 mT, from the solenoid was present when transition occurred the shield would trap this field with a resulting increase in noise.

The N.M.R. spectrum could be obtained by slow or fast passage techniques.

For a slow passage, the frequency output of the generator was internally swept between predetermined end points. The X axis of the X-Y recorder was driven by the sweep output of the generator. The Y axis was connected to the lock-in output of the SQUID electronics.

For the experiments on the copper wire bundle, the X axis was a linear function of frequency. Resonance frequencies were determined by manually changing the frequency until the SQUID signal was maximum. The frequency at which this maximum occurred was measured by a frequency counter.

The r.f. power level of the generator was increased until the resonance signal was maximized. The amount of A.C. current flowing in the N.M.R. r.f. coil was determined by measuring the voltage drop across an 83.3 ohm, carbon resistor in series with the coil.

In the fast passage technique, a continuous triangular wave signal was applied to the X axis of the recorder. The zero of this axis was shifted to the center. The pen oscillated about the zero, with an amplitude controlled by the auxillary function generator supplying the triangular wave. To obtain measurements of τ_1, the Waveteck 144 generator was set up for a single sweep, at an appropriate rate, through a range sufficiently wide enough such that the end points were far from resonance. Once the triggered sweep was completed, the output frequency of the generator returned to the original starting point. The resulting trace displayed the magnetization of the sample as a function of time as the pen moved back and forth across the paper. The tracing displayed in Fig. (12) is typical of the spectra obtained in this manner.

The resonance frequency was determined, by frequency modulating the generator and using the sweep output to drive the X axis of the recorder. The amplitude and the period of the modulating signal were adjusted to insure A.F.P. requirements. If the base line is steady i.e. no drift in the SQUID electronics output, the resonance frequency will be the intersection point of the risers. This point should be midway, corresponding to M_z equal to zero. An ideal case is represented in Fig. (13). If the reversal of magnetization is not quite complete the intersection point should still be the resonance frequency given by $|\omega_0| = |\gamma B_0|$.

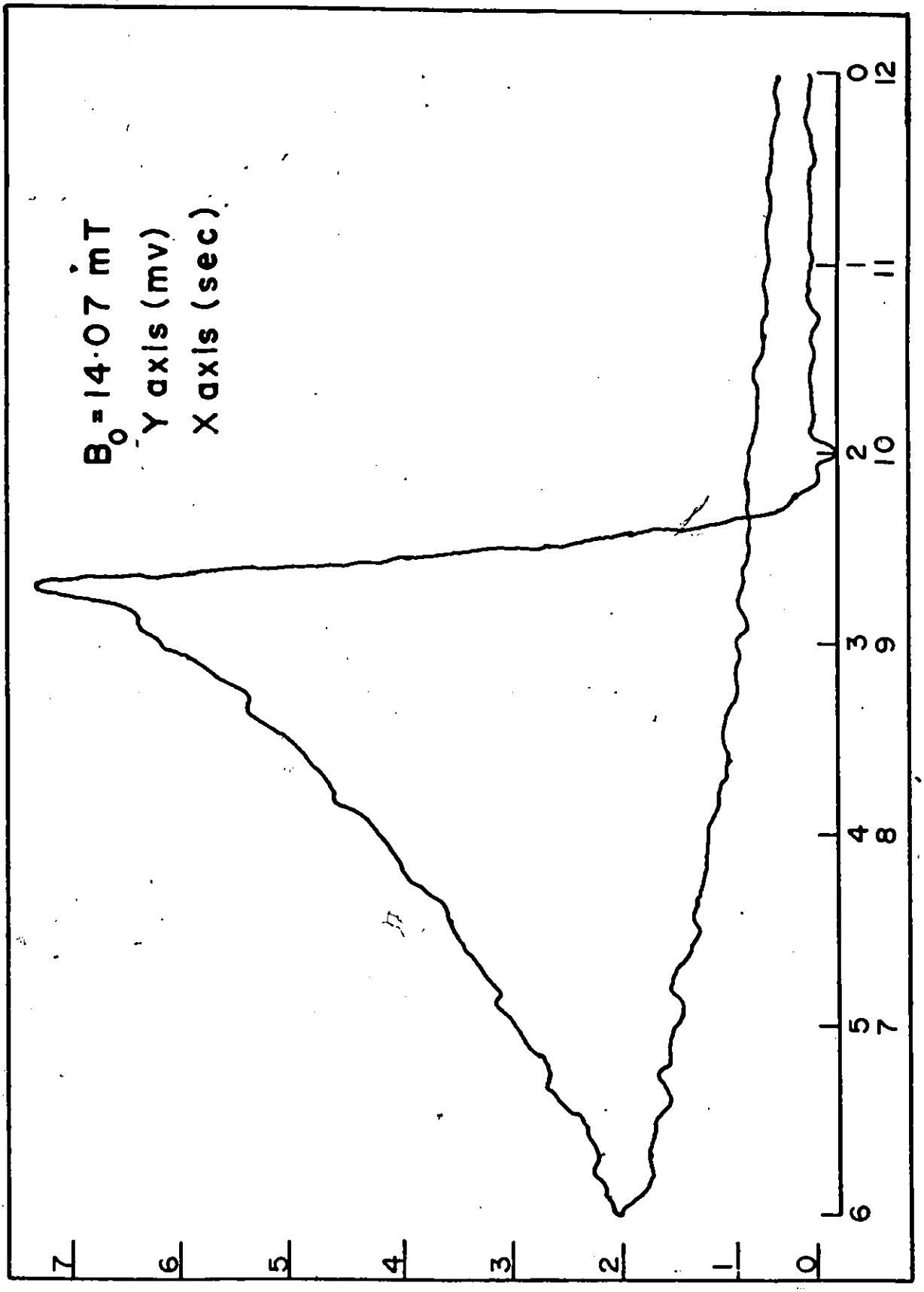
B_o = 14·07 mT
Y axis (mv)
X axis (sec)
0 12
1 11
2 10
3 9
4 8
5 7
6
7
6
5
4
3
2
1
0

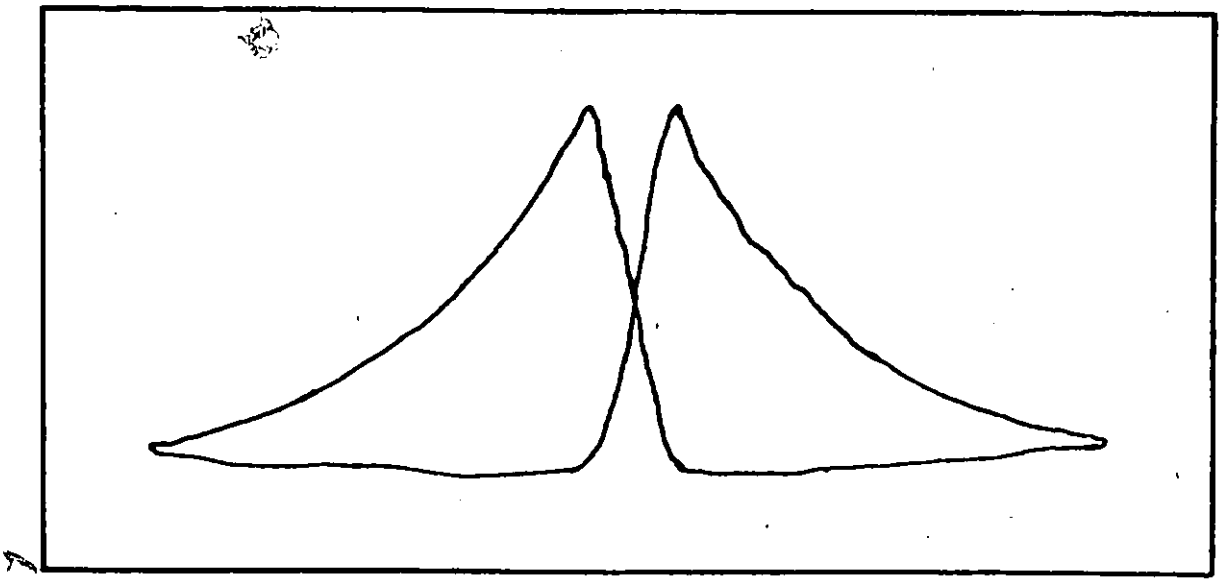

Figure 13. Ideal A.F.P. tracing for field determination.

CHAPTER III

INTRODUCTION

This Chapter deals deals with the preliminary investigations into the use of the S.M.-N.M.R. signal amplitude of Cu^{63} for the purpose of thermometry. The signal observed in slow passage is, for a given magnetic field, not only a function of temperature, but also of the amplitude of the r.f. field (28).

In the experiments reported herein, the behaviour of the signal size was studied as a function of B_1, at a constant temperature (4.2K) and in a fixed field B_o (30.63 mT).

The sample was a bundle of 5900, #46 A.W.G. insulated copper wires. The bundle was packed inside a delrin tube (0.550 cm I.D., 0.646 cm O.D.) on which the r.f. saddle shaped coils were placed. The amount of copper enclosed by the volume of the coils (1.4 cm x 0.24 cm^2) was estimated to be 0.94 grams (0.65 grams Cu^{63}, 0.29 grams Cu^{65}). Assuming that the profile of the field trapped is that of the liquid N_2 cooled solenoid, the field inhomogeneity over the sample is calculated to be 93 μT/4.32 mT, where 4.32 mT is the field produced in the solenoid by a current of 1 amp.

The gradiometer, was wound such that the two coils comprising it, were 3.3 cm apart and situated 4.55 and 7.85 cm, respectively, from the bottom end of the field trap. From the previous assumption, we obtain a field difference of 66 μT/4.32 mT.

The superconducting field trap maintains a constant flux over its interior cross-sectional area A_T. A flux change $\Delta\Phi = A_S \Delta M$, produced by a change of magnetization of a sample (cross-sectional area A_S), results in a corresponding change, $-\Delta\Phi$, in the annular area not occupied by the sample, i.e. in the annular region defined by $A_T - A_S$, and is a consequence of a change of the currents flowing on the inside surface of the superconducting trap to keep the net flux constant (Fig. (14)). Thus, if the sample does not fill the pick-up coil, the resulting signal from $\Delta\Phi$ will be reduced by the amount of the negative flux change enclosed by the coil.

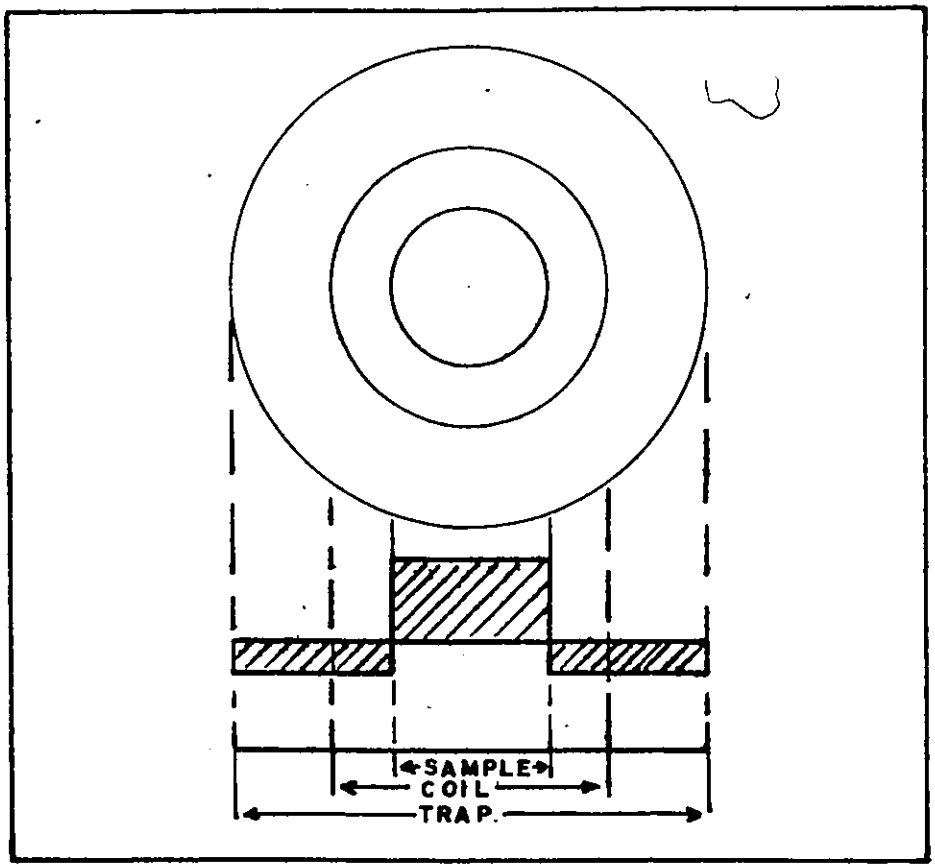

Figure 14. Sectional schematic of sample, transformer and trap.

Here, the cross-sectional area ratios of the sample and sample coil, to the field trap, expressed in percentages, were 10.8 and 34.4 respectively. Thus we have a theoretical signal reduction of 26.5% because of the geometry.

EXPERIMENTAL RESULTS

The tracing in Fig. (15), is a typical N.M.R. spectrum for Cu^{65} and Cu^{63}. The drift in the baseline was generally observed in all runs. The signal-to-noise ratio, typically 7:1 for saturated signals, was approximately 5:1 for lower r.f. powers.

Line width measurements, taken from recordings of saturated Cu^{63} signals at two fields (33.94 and 30.2 mT) yielded (4.4 and 4.3 ± 0.5 kH_z or 0.39 and 0.38 ± 0.04 mT) respectively.

For the study of the behaviour of the signal size as a function of B_1, a standard carbon resistor was placed in series with the r.f. coils. The alternating current in the circuit was found by measuring the voltage drop across this resistor at the N.M.R. resonance. Thus, from the estimated field factor of the saddle coils (0.97 mT/amp), the amplitude of the r.f. field B_1, could be determined. Several spectra of Cu^{63} were taken for each value of B_1. The maxima of the Cu^{63} signal were averaged to obtain a value of the amplitude at that particular value of B_1. The data were expressed as a percentage of the saturated value of 1.1 mv.

Equation (28) can be written in the following form

$$A = \frac{cB_1^2}{T(T + bB_1^2)} \qquad (35)$$

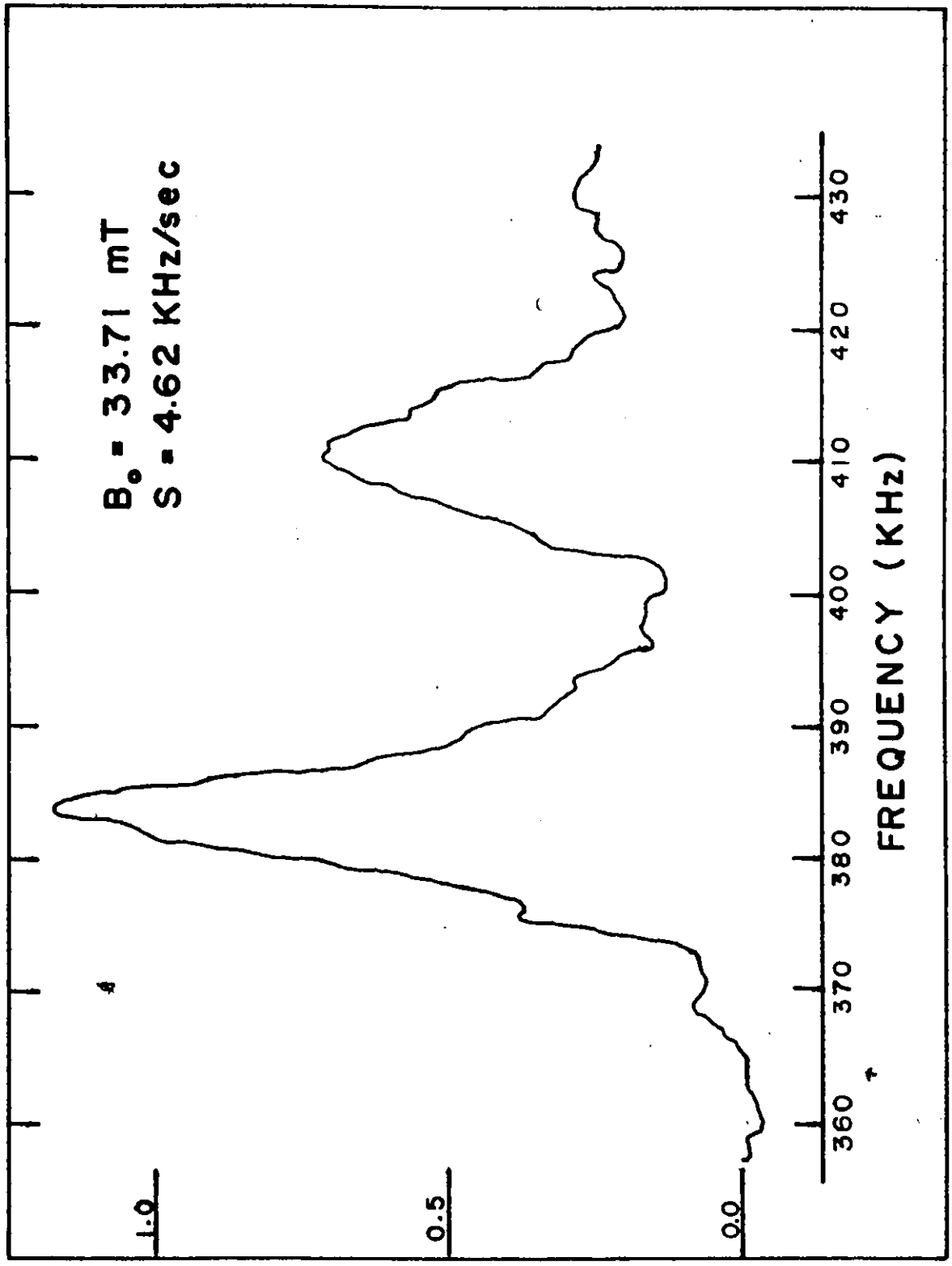

FIGURE (15) N.M.R. SPECTRUM OF Cu^{63} & Cu^{65}

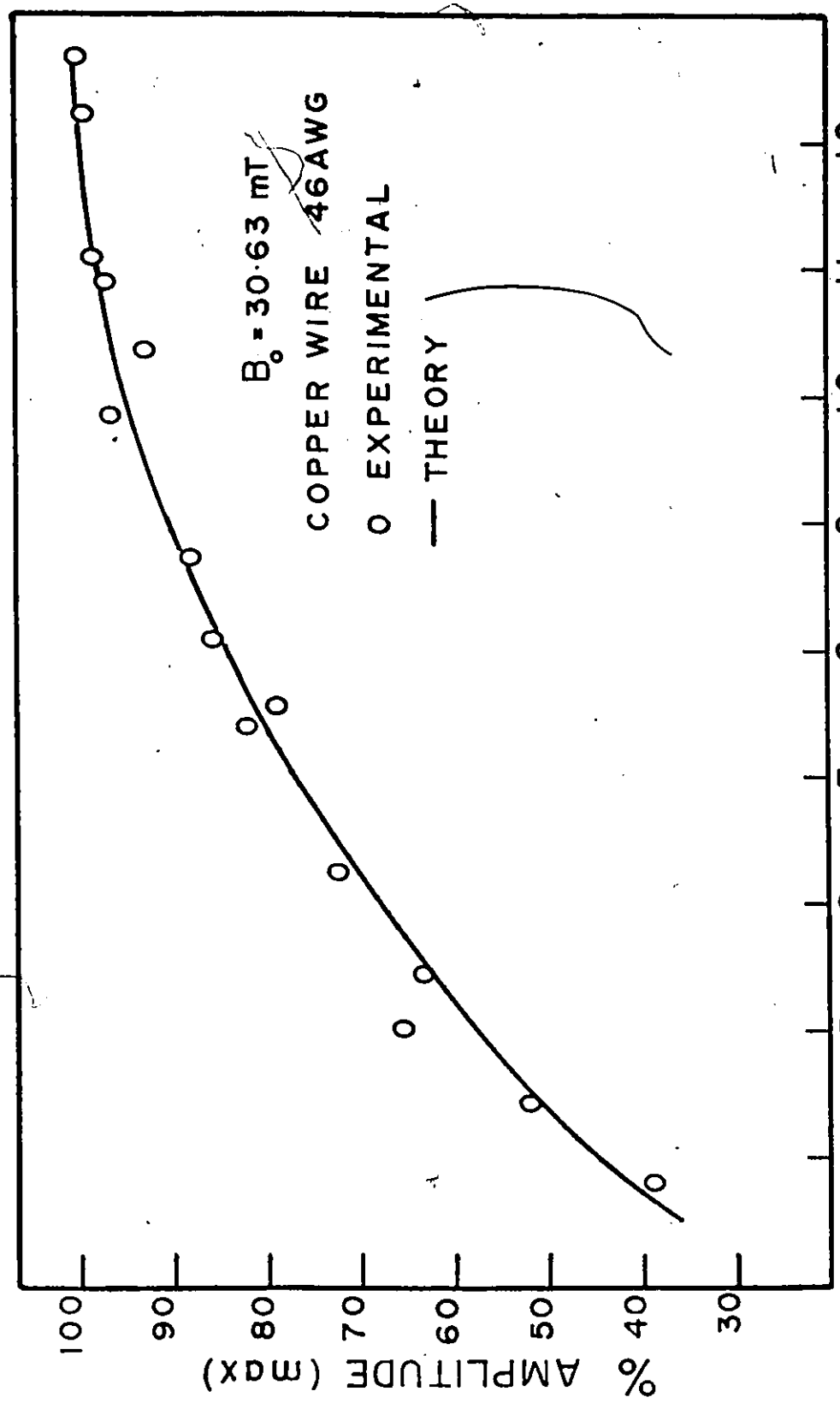

Graph (3). Percentage of saturated signal amplitude vs r.f. field amplitude.

This equation may be rewitten in a form that is amenable to a least-squares analysis. Doing so we obtain

$$\frac{1}{A} = \frac{a}{B_1^2} + d \qquad (36)$$

where $a = T^2/c$, $d = bT/c$ and B_1 is expressed in μT. Using the experimental data obtained in a field of 30.63 mT, at 4.2 K, the parameters, a and b, were found to be 23.4 and 0.819, respectively. The experimental data, compared to a curve derived from (32), using for c and b, 0.754 and 0.147, respectively, is displayed in Graph (3). The error on the measured amplitudes is typically 15%

DISCUSSION

The measured line widths were found to be of the order of the known natural line width in metallic copper (0.3 mT[15]) indicating that the field trapped in the niobium cylinder was fairly homogenous. One is drawn to the conclusion that the field maintained by the trap is much more homogeneous than the original field generated by the solenoid and later trapped. Indeed if the field profile within the trap was that of the solenoid, then the line width would have been around 1.0 mT. Thus, the astatic coils of the gradiometer are situated in a field difference much smaller than 66 μT/4.32 mT.

The behaviour of the N.M.R. signal amplitude of Cu^{63}, as a function of B_1 is in agreement with theory. The values of B_1, estimated from equation (33) are considered to be approximate. A calculation of

the saturation factor, $(\gamma^2 B_1^2 \tau_1 \tau_2)/(1 + \gamma^2 B_1^2 \tau_1 \tau_2)$ indicates that the approximation is quite good. The calculated saturation factor is 92% for that value of B_1 (12.68 μT) where, experimentally, saturation was observed.

Recent experiments in our laboratory on S.M.-N.M.R. have demonstrated that the reduction of the noise level observed for a gradiometer system, as opposed to a single coil, is not significant enough to justify the use of the former. Since the self-inductance of a coil is proportional to the square of the number of turns, by using a single coil and maintaining the same self-inductance as for the gradiometer, it should be possible to obtain an increase of 1.4 in the flux transfer factor (if N is the number of turns on the pick-up coil of the gradiometer then the number of turns on the single coil for the same self-inductance, becomes 1.4N). The flux transfer factor can also by better matching of inductances be increased by at least a factor of 2. Indeed, the figure of 0.015 quoted for this work could be quite erroneous in that the sum of the self-inductance of the gradiometer (or single coil) and leads, should never exceed the self-inductance of the signal coil. An error in measurement of the inductance of the gradiometer used in this work, resulted in a very bad mismatch.

Thus, it should be possible to obtain: (1) larger signals (at least 3 x) as indicated in the previous discussion, and (2) a reduction in the noise level by (a) securing the magnetometer more firmly and (b) using stainless-steel dewars for shielding. Having achieved the above, the signal-to-noise ratio would be 40 - 1 or better.

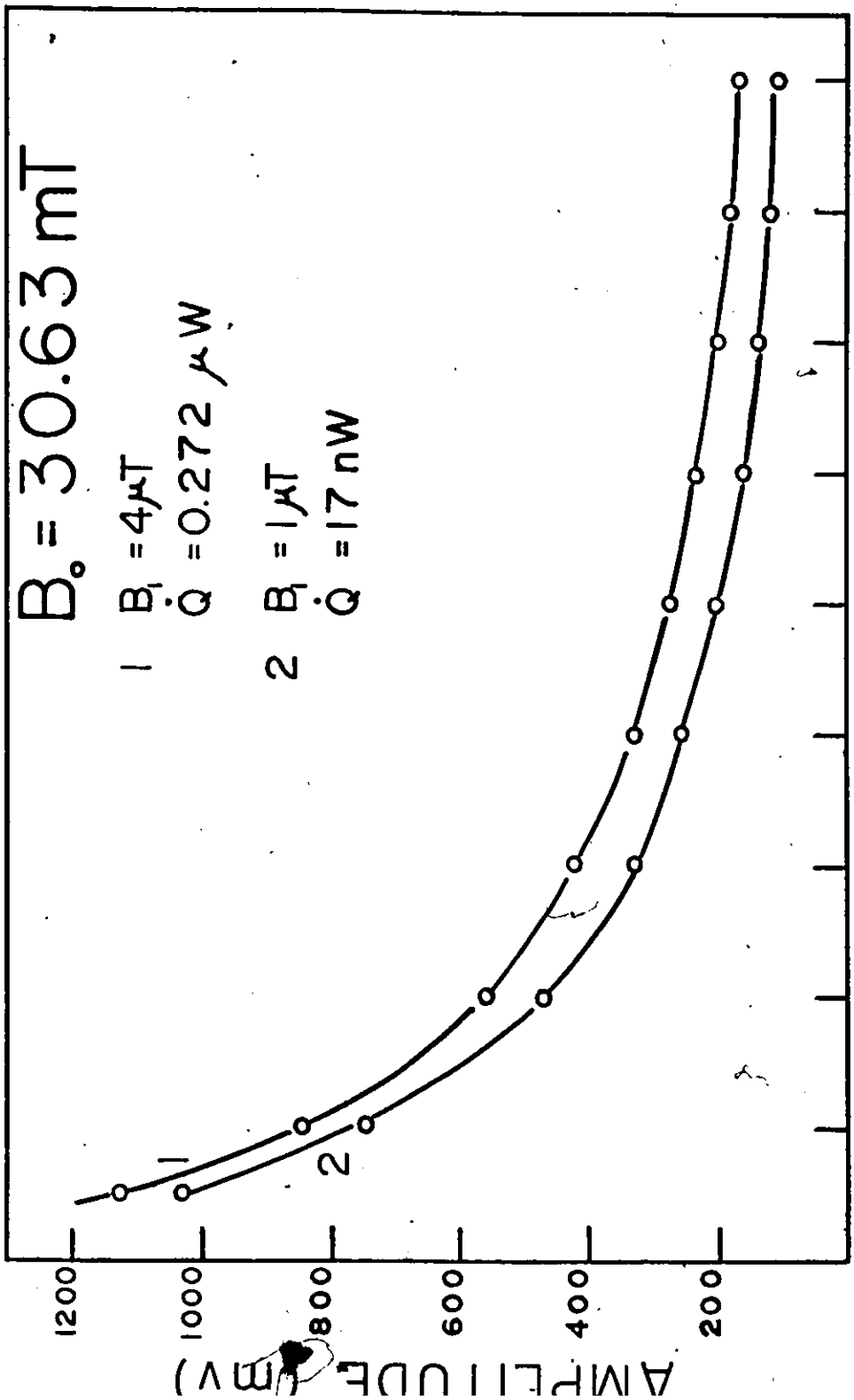

Graph (4). Expected N.M.R. amplitude of Cu^{63} as a function of r.f. amplitude and temperature.

Using the values for c and b, the amplitude as a function of temperature can be calculated for various constant values of B_1 (assuming an increase of 3 x in saturated signal). In Graph (4), two curves, corresponding to B_1 = 4μT and 1μT respectively, are shown for the temperature region of 10-100 mK. The eddy current heating 1.5 in the Cu wire bundle, for B_1 = 1μT, is 1.7 x 10^{-8} Watts (0.17 ergs/sec). By reducing B_1 to 0.1μT, the heat input drops to 1.7 x 10^{-10} Watts (1.7 x 10^{-3} ergs/sec) and the amplitude at 10 mK becomes 217 mv (for B_1 = 1μT, at 10 mK, A = 1.585 volts!). This amplitude of 217 mv is entirely adequate for thermometry in this range. In fact, at 1 mK the expected signal amplitude would be 10.074 volts!

For the saddle coil used here, the field B_1 of 0.1 μT corresponds to an r.f. current of 72.8 μA. To estimate the fluctuation allowable in this current, consider equation (32). For a given amplitude A, an uncertainty in B_1, of ΔB_1, will result in an uncertainty ΔT in the temperature. The relative errors are related by,

$$\frac{\Delta T}{T} \simeq \frac{\Delta B_1}{B_1} \left(\frac{2T}{2T + bB_1^2} \right) \tag{37}$$

For there to be an uncertainty of only 1% at 10 mK, in T (B_1 = 0.1 μT), the corresponding uncertainty in B_1 must be at most 1.1%. Thus the fluctuation allowable in the r.f. current is also 1.1% or 8 μA for this example. For an error of 1.1% in B_1 at 10 mK, the resulting relative change in signal amplitude can be determined from

$$\frac{\Delta A}{A} = \frac{\Delta B_1}{B_1} \left[\frac{2T^2}{(T^2 + bTB_1^2)} \right] \tag{38}$$

and is found to be 2.2%.

Thus, if precautions are taken to insure a stability in the r.f. current of at least 1%, it should be possible to determine the temperature with an error of less than 5%.

Though it should be fairly easy to obtain an accurate temperature measurement, care must be taken to insure that the thermometer is in thermal equilibrium with the sample being monitored. For example, if the thermal boundary resistance R_K between the thermometer and the sample is of the Kapitza type ($R_K \alpha 1/DT^3$, D is the contact area) then the response time of the thermometer is not τ_1 but[15]

$$\tau = (\tau_1 + R_K C_N) \qquad (39)$$

Here, C_N is the heat capacity of the nuclear spins and is assumed to be very much larger than C_e (electronic heat capacity), but much less than the sample heat capacity.

Since the thermometer is heated as previously discussed, equilibrium will be destroyed as this heat input will cause a thermal resistance due to the temperature gradient set up at the thermometer-sample boundary. To reduce the time required for equilibrium to be re-established, the contact area can be increased and the r.f. power level reduced, thereby diminishing ΔT at the boundary.

However, if A.F.P. is used and the requirements for adiabaticity are met, then a measurement of the temperature can be obtained in a few seconds. The signal amplitude as previously mentioned is a function of 1/T and would be greater than the A.S.P. signal by $\frac{2\,(1 + \gamma^2 B_1^2 \tau_1 \tau_2)}{\gamma^2 B_1^2 \tau_1 \tau_2}$. The main feature is the short time that the spin

system is irradiated, as compared to A.S.P. The signal is then a measure of the sample temperature providing the sample and thermometer were in equilibrium prior to the introduction of the r.f. field.

For a field B_1 of 4μT, the A.S.P. maximum at 10 mK is calculated to be 1.685 volts! The A.F.P. signal would be a factor of 2 greater. The heat input, though would be 2.7 ergs/sec, which could possibly be intolerable. One problem with such a large amplitude is that the SQUID might be unable to follow the change. This SQUID system can accommodate a rate of change of 250 Φ_0/sec, which corresponds to an output voltage change of 10 volts/sec. Thus to insure an accurate temperature measurement, the rate of change of flux must be kept below the maximum allowable rate.

CHAPTER IV

INTRODUCTION

The long relaxation times, τ_1, usually encountered for the F^{19} spin system in CaF_2 make this crystal ideal for study by A.F.P. The relaxation times are field dependent and are strongly influenced by impurities. S. Day et al,[19] report values of τ_1, ranging from about 8 - 22 seconds, for fields of 10.0 - 30.0 mT, for a CaF_2 sample containing Fe^{++} (1ppm).

In the work reported here, a sample of CaF_2 (Materials Research Corporation) was studied by the fast passage method previously described, in fields from 3 - 30.0 mT.

At low fields, the resonance signal produced by the delrin sample tube (Chapter III) would be quite close to the fluorine resonance signal. For example, at 10.0 mT the proton resonance is at 425.76 KHz, whereas the fluorine resonance is at 400.55 KHz, a difference of only 25.21 KHz. The signals would overlap because of the line widths of the two signals. To avoid this problem, a thin walled quartz tube (0.67 cm I.D., 0.736 cm O.D.) was substituted for the delrin tube and a suitable r.f. coil was positioned on it.

The gradiometer coils were 4.21 cm apart and situated 4.01 and 8.22 cm respectively from the lower end of the field trap.

The cross-sectional area ratios of the sample coil and sample to the field trap, expressed as percentages, were 34.4 and 16.1 respectively, an improvement in the latter case of 15.4% over the previous arrangement.

SAMPLE

A 0.94 gram rectangular parallelopiped was cut from a cube of CaF_2, 1 cm on edge, with a circular diamond saw. This was then shaped, using fine emery paper, into a cylinder, 0.67 in diameter by 1 cm in height. The (111) direction (along the length) was oriented parallel to the trapped field. The surface of the sample was uneven and very rough.

The sample was washed in acetone, distilled water, and then a 10% solution (by volume) of H_2SO_4 for 15 minutes. The cylinder was then rinsed thoroughly in distilled water, dried by evaporation and sealed in a quartz ampoule, partially filled with helium. The ampoule was then placed in a furnace and the temperature raised to 600^oC in about 4 hours. The sample remained in the furnace at this temperature for 70 hours, at the end of which, it was cooled to room temperature in 5 hours. The surface of the CaF_2 cylinder, previously milky white, was considerably smoother and clearer.

EXPERIMENTAL RESULTS

The tracing in Fig. (16) is a typical N.M.R. spectrum of F^{19}, produced by A.F.P. at 3.76 mT. The signal-to-noise ratios were generally better than 40-1. Line width measurements were obtained from the tracings used to determine the field. The width was taken to be the distance between the beginning of the riser and the maximum. As the line widths, demonstrated no appreciable dependence on field, the measurements were averaged together. For example the widths at 8.86 and 18.14 mT were 0.77 ± 0.06 mT and 0.8 ± 0.05 mT respectively. Thus, the average line width was found to be 33 ± 2KHz, or 0.82 ± 0.05 mT.

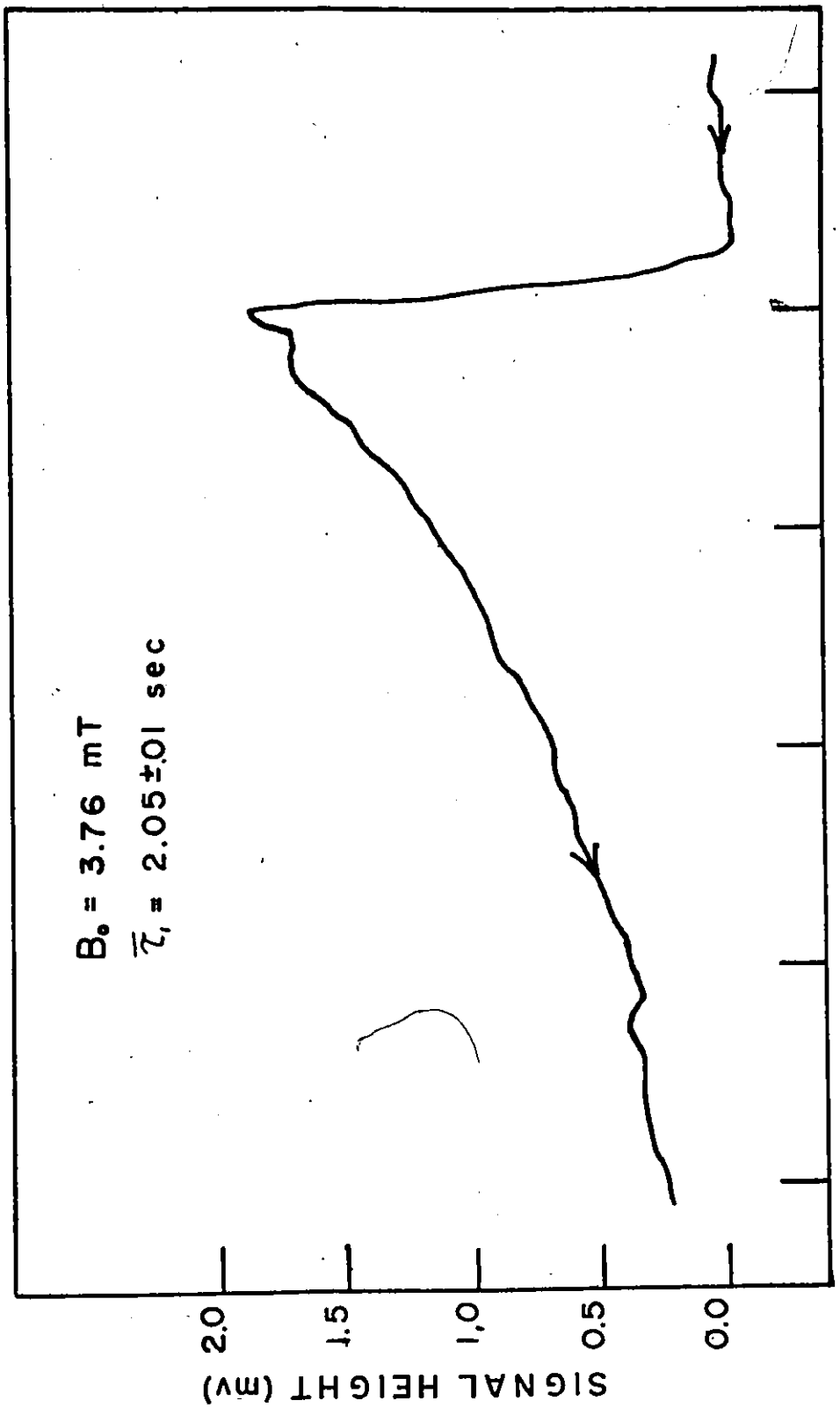

Figure 16. Typical F^{19} tracing (A.F.P.).

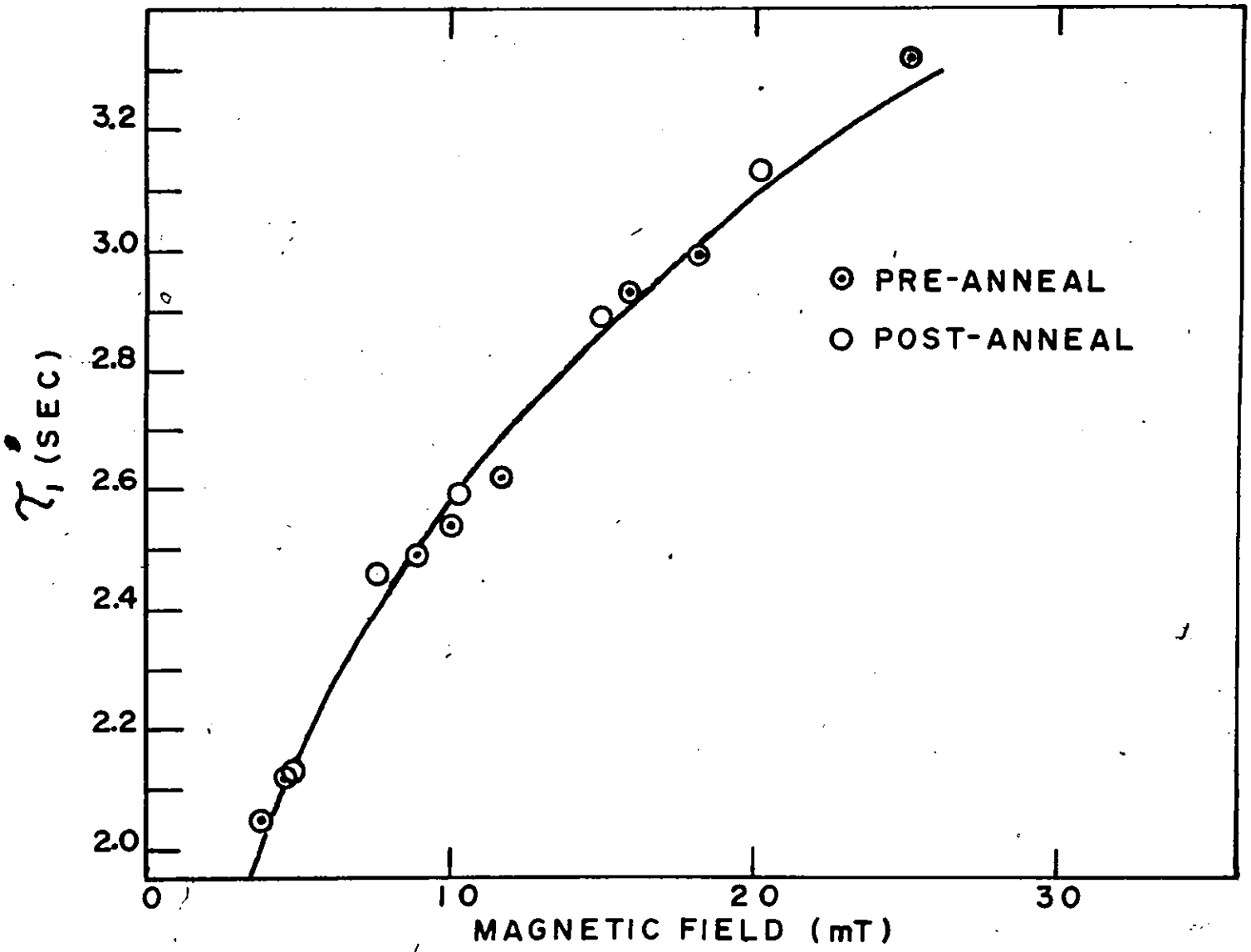

Graph (5) Relaxation time of F^{19} as a function of magnetic field.

A small hydrogen signal (about 8% of the F^{19} signal amplitude) was observed in the tracings used for field determination Fig. (17). The relaxation time for this signal was short compared to τ_1 for F^{19}. However to avoid any problems, the frequency range for fast passage was adjusted to exclude the proton signal.

Measurements of τ_1 of F^{19} in CaF_2 were made before and after annealing. No change in τ_1 was observed for the same applied magnetic field. Thus all results were incorporated together. The relaxation times were found to be shorter than those reported by S. Day et al. At 30 mT τ_1 was 3.4 seconds compared to their 22 seconds.

A logrithanic least-squares analysis of the data, showed the field dependence of τ_1 to be

$$\tau_1 = 1.439 \cdot B_o^{0.255} \qquad (40)$$

where B_o is expressed in mT. The data, separated into pre and post anneal is presented in Graph 5. The solid curve is derived from equation 40. Each τ_1 is an average of a minimum of twenty measurements for each values of B_o. The uncertainty in τ_1 was typically 5%.

Such small relaxation times indicate the presence of an impurity in a concentration greater than 1 ppm. To ascertain if this was so, a room temperature E.S.R. spectra was taken of the sample. The spectra bears a strong resemblance to that of manganese.[20] Unfortunately, no standard spectra were available for comparison. We were thus unable to determine the impurity concentration.

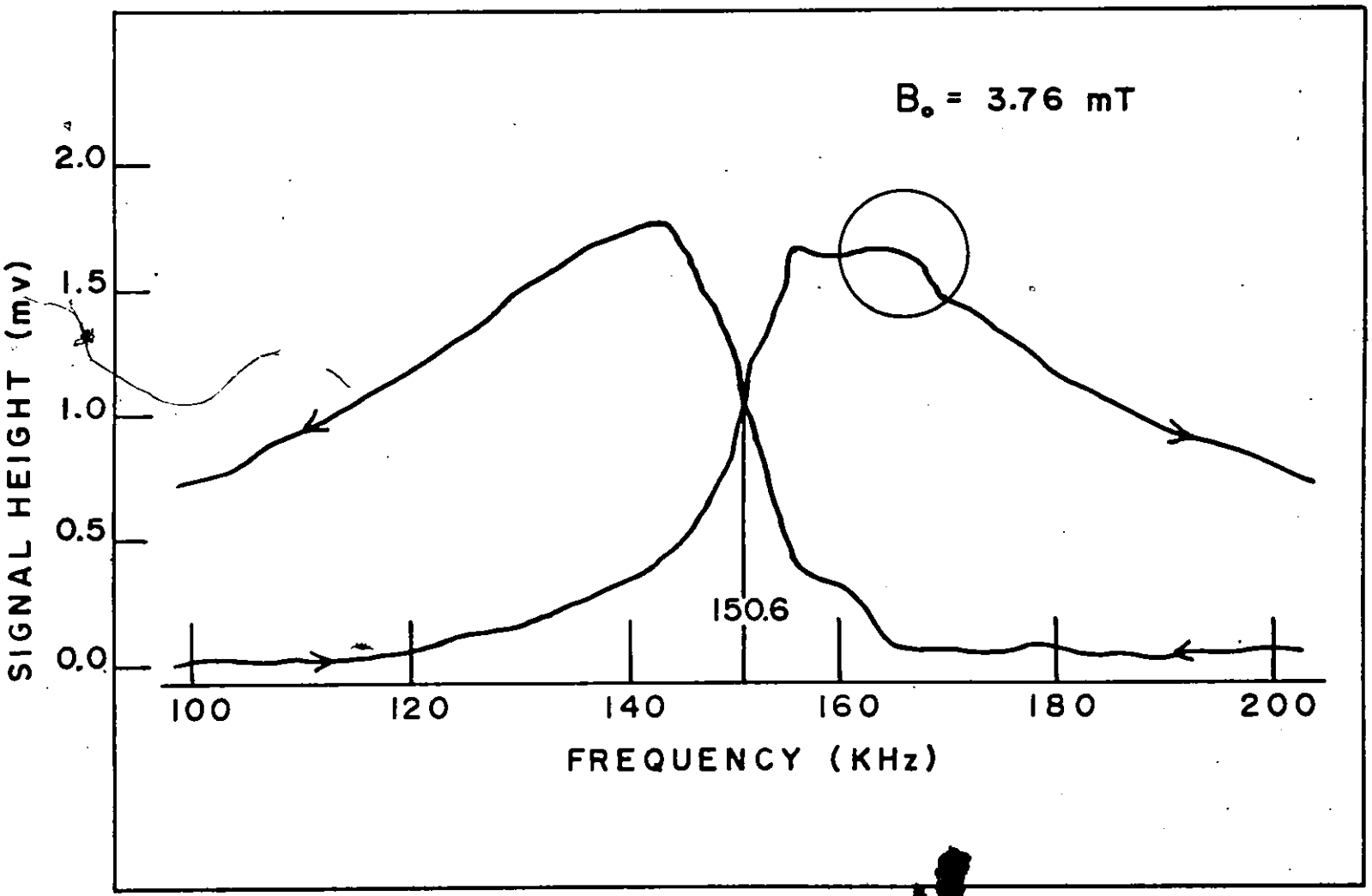

Figure 17. Field determination tracing - F^{19} signal (hydrogen signal circled).

DISCUSSION

As no saturated slow passage measurements were performed, we are unable to indicate if the A.F.P. spectra do indeed give a factor of 2x in signal amplitude. It would be good procedure to compare both signals as a means of insuring that A.F.P. requirements are met. However, the signal maxima may be reduced, in that the X,Y recorder can only follow changes less than 12 cm/sec. Typically for this work, the velocity in the Y direction was 25 cm/sec. Thus, though the signal may be maximized, the recorded amplitude would not be twice the slow passage signal.

The measured line widths agree, within the experimental error, with the value of 0.8 mT reported by Hatton and Rollin.[21] Again, one is drawn to the conclusion that the field in the superconducting trap is fairly homogeneous.

The hydrogen signal is quite probably due to the masking tape securing the r.f. coil. As the signal appears to be a broad slow passage line Fig. (17) it can be inferred that the relaxation time of the protons is much less than one second.

In a crystal such as CaF_2, the relaxation time, τ_1, is strongly influenced by the presence of paramagnetic impurities. For pure crystals τ_1 is expected to be very long, as the transfer of energy, absorbed from the r.f. field, is limited to the process of spin diffusion. This is a random walk process, due to the weakness of the spin-spin interaction, which involves the simultaneous directional reversal between a pair of anti-parallel spins. N. Bloembergen[22] has shown that the energy absorbed by the F^{19} nuclei at one end of a pure 1 cm long CaF_2

crystal, would take 10^{12} seconds to reach the other end in an amount sufficiently large enough to effect the spin temperature. For an impure cyrstal, the model proposed by Bloembergen, consists of a distribution of 'heat sinks'. The heat sink is a sphere of F^{19} nuclei, at the center of which is a paramagnetic impurity. The impurity nucleus produces a strong local magnetic field gradient which is active over a critical radius b. At this distance, the field produced by the impurity is about equal to the local field produced by the other nuclei. The nuclei inside this radius will have shorter relaxation times, but their resonance frequencies are shifted to the wings of the resonance line. The F^{19} nuclei in the shell outside the impurity sphere will exchange energy by the diffusion process. Once the energy crosses the boundary it is quickly exchanged with the lattice. The thickness of the shell is determined by the impurity concentration and the uniformity of distribution.

The diffusion process is completely independent of both the temperature of the lattice T_ℓ and the external field B_o. However, the heat contact with the lattice via the impurities is a sensitive function of T and B_o.

S.M. Day et al[19] have shown that the field dependence of the relaxation time of F^{19} in CaF_2, for a uniformity distributed impurity, in the low field approximation, $\mu B_o/kT \ll 1$, may be expressed as

$$\tau_1 \alpha ((1 + \rho^2/\ ^2)/\rho)\chi^{0.75} \qquad (41)$$

for the rapid diffusion case (i.e. many heat sinks or high impurity

concentration); and for the diffusion limited case

$$\tau_1 \alpha \left((1 + \rho^2 \nu^2)/\rho\right)^{0.25} \tag{42}$$

Here, $X \equiv \mu B_0/kT$, ρ is the impurity spin lattice relaxation time and ν is the resonance frequency of the fluorine nuclei.

If $\rho\nu$ is less than 1, we observe that the relaxation time may be written, for constant temperature, as

$$\tau_1 = f B_0^{\sigma} \tag{43}$$

where f is a constant of proportionality and τ is an index ranging from 0.75 to zero.

Thus, our result of $\tau_1 \alpha B_0^{0.255}$, would indicate that at 4.2K, the relaxation time for F^{19} in this crystal, lies somewhere between the two previously mentioned cases.

CHAPTER V

CONCLUSIONS

An N.M.R. magnetometer using a SQUID has been constructed and measurements on metallic copper and a sample of CaF_2 have been performed. The device is very dependable as well as being simple to operate. The simplicity lies in the fact that the N.M.R. signal is detected directly as a change in magnetization and one therefore is not burdened with tuning the r.f. coil circuit as is the case in standard N.M.R.

Using this magnetometer, the dependence of the amplitude of the Cu^{63} resonance signal, on the r.f. field amplitude was investigated. This dependence was found to be, at 30.63 mT

$$A = \frac{0.754\ B_1^2}{17.64 + 0.617\ B_1^2}$$

and was of the form predicted by theory. Also measurements of the line width yielded 0.39 and 0.38 ± 0.04 mT for fields of 33.94 and 30.2 mT, respectively. The previously published value is 0.3 mT. This indicates that the magnetic field inhomogeneity over the length of the sample is very slight (0.3% of field), in the region where the sample is located.

The magnetic field dependence of the relaxation time of the F^{19} nuclei in a CaF_2 sample, was investigated with this magnetometer. It was found that for the field range of 3.0 mT to 30. mT, the relaxation

time was given by

$$\tau_1 = 1.439\ B_o^{0.255}$$

Line width measurements yielded 0.82 ± 0,05 mT which is in good agreement with the previously published value of 0.8 mT.

The very small field inhomogeneity of the field trap, indicates that the profile of the applied field is not trapped by the superconducting cylinder. It would be of interest to construct a very small N.M.R. probe and map the field inside a cylinder as a function of position as well as for various profiles of the applied field.

As indicated by the discussion in Chapter III, the realization of a nuclear magnetic thermometer of at least 5% accuracy, using a SQUID magnetometer, is quite feasible. However, changes in the magnetometer head would be necessary. The head would have to be thermally anchored at a constant temperature to avoid magnetic noise from those materials comprising it, which would be magnetized. This would necessitate thermally isolating the copper sample from the magnetometer. The r.f. shield would have to be constructed from some material other than copper (silver, etc.) as the present shield would contribute to the resonance signal amplitude and in the new head would not necessarily be at the same temperature. To increase the signal amplitude, the sample filling factor as well as the flux transfer factor would have to be increased. The former would present a problem in that the r.f. coil would be in very close proximity to the shield walls. This could result in distortion of the r.f. field as well as some leakage to the transformer coil. To avoid any difficulty a simple circular coil of several turns would be substituted for the

present r.f. coil. (Recent experiments in this laboratory using this geometry have been quite successful.)

The latest SQUID system marketed by S.H.E. is extremely stable. The model 202 was adequate for the study of long relaxation times by A.F.P. This new system (model 330) would permit measurements at fields lower than 3 mT.

SQUID N.M.R. is no longer a mere curiosity and with further work it will undoubtedly become a standard method for N.M.R. work at low fields.

BIBLIOGRAPHY

1. a) S.H.E. Corporation, 1161 Sorrento W. Rd., San Diego, California 92121, U.S.A.
   b) Develco Inc., 530 Logne Avenue, Mountain View, California 94040, U.S.A.
   c) Canadian Thin Films Ltd., 3168 Lake City Way, Burnaby, British Columbia, Canada
2. D. Cohen, Science, Vol. 175, page 664, (1972).
3. A. Rosen, G.T. Inouye, A.L. Morse and D.L. Judge, J. Applied Phys., 42, 3682 (1971).
4. J.E. Zimmerman and N.V. Frederick, Appl. Phys. Lett., 19, July 1971.
5. E.C. Hirschkoff, O.G. Symko, L.L. Vant-Hull and J.C. Wheatley, J. Low Temp. Phys., 2, 653 (1970).
6. R.E. Walstedt, E.L. Hahn, C. Froidevaux and E. Geissler, Proc. of the Royal Society, A. 284, 499 (1965).
7. E.P. Day, Phys. Rev. Lett., 29, 540 (1972).
8. D.J. Meredith, G.R. Pickett, O.G. Symko, Phys. Lett., 42A, 13 (1972).
9. G. Lamarche, B. Hebral, G. Goodchild, Unpublished work on Delrin and CaF_2 (1972).
10. E.J. Cukauskas, D.A. Vincent, B.S. Denver Jr., Rev. Sci. Instrum., Vol. 45, 1, 1, 1974.
11. O.V. Lounasma, Experimental Principles and Methods Below 1K, Academic Press Inc., London (1974).

12. S.H.E., Manual for Superconducting Quantum Electronic System Model 202.

13. M.W. Zemansky, Heat and Thermodynamics, 5th ed. (1968) McGraw-Hill).

14. A. Buhrman, W.P. Halperin, S.W. Schwenterly, J. Reppy, R.C. Richardson and W.W. Webb, Proc. of 13th Low Temp. Phys. Conference, Tokyo, 1970.

15. O.G. Symko, Temperature - Its Measurement and Control in Science and Industry, Vol. 4, Part 2, page 1239, 1972.

16. A. Abragam, The Principles of Nuclear Magnetism, 1961, Oxford.

17. D.J. Meredith, G.R. Pickett, O.G. Symko, J. Low Temp. Phys., 13, 607 (1973).

18. H.E. Duckworth, Electricity and Magentism. (Holt, Rinehart, Winston) (1960) page 206.

19. S.M. Day, E. Otsuka, B. Josephson, Jr., Phys. Rev. 137, 108 (1965).

20. A. Manoogian (Private communication).

21. J. Hatton and B.V. Rollin, Proc. Roy. Soc., London, 1949, A199, 222.

22. N. Bloembergen, Physica XV, 1949, 386.